Electronic Supplementary Information (ESI)

Synthesis, Characterization, and Reactivity Studies of Electrophilic Ruthenium(II) Complexes: Study of H_2 Activation and Labilization

K. S. Naidu, Yogesh P. Patil, Munirathinam Nethaji and Balaji R. Jagirdar*

Department of Inorganic & Physical Chemistry, Indian Institute of Science, Bangalore 560012, India

Contents:

Figure S9. (a) ORTEP view of [RuCl(OH_2)(bpy)(dfppe)] cation (**9**) and selected bond lengths and bond angles; (b) ^{1}H NMR spectrum of (**9**); (c) ^{31}P{^{1}H} NMR spectrum of (**9**); (d) ^{19}F NMR spectrum of (**9**) (e) ES-MS spectrum of (**9**)

Figure S10. (a) ORTEP view of [RuH(PMe_3)(bpy)(dfppe)] cation (**10a**) and selected bond lengths and bond angles; (b) ^{1}H NMR spectrum of (**10a**); (c) ^{31}P{^{1}H} NMR spectrum of (**10a**); (d) ^{13}C NMR spectrum of (**10a**); (e) ES-MS of spectrum (**10a**)

Figure S11. (a) ^{1}H NMR spectrum of [RuH($P(OMe)_3$)(bpy)(dfppe)][OTf] (**11a**); (b) ^{31}P{^{1}H} NMR spectrum of (**11a**); (c) ^{13}C NMR spectrum of (**11a**); (d) ES-MS spectrum of (**11a**)

Figure S12. (a) ORTEP view of [RuH($P(OMe)_3$)(bpy)(dfppe)] cation (**11c**) and selected bond lengths and bond angles; (b) ^{1}H NMR spectral stack plot (acetone-d_6, 293 K) indicating the isomerization of (**11a)** to (**11c**); (c) ^{31}P{^{1}H} NMR spectral stack plot indicating the isomerization of (**11a)** to (**11c)**

Figure S13. (a) VT ^{1}H NMR (CD_2Cl_2) spectral stack plot for the reaction of [RuH($P(OMe)_3$)(bpy)(dfppe)][OTf] (**11a)** with HOTf; (b) VT ^{31}P{^{1}H} NMR (CD_2Cl_2) spectral stack plot for the reaction of (**11a)** with HOTf; (c) VT ^{31}P{^{1}H} NMR (CD_2Cl_2) spectral stack plot for the reaction of (**11a)** with HOTf; (d) VT ^{19}F NMR spectral stack plot for the reaction of (**11a)** with HOTf; (e) Spin-saturation transfer experiment: ^{31}P{^{1}H} NMR spectral stack plots for the reaction of (**11a)** with HOTf (irradiation of **13a**)

Figure S14. (a) ^{1}H NMR spectrum of isomeric aqua complexes (**14a**, **14b**) [Ru(H_2O)($P(OMe)_3$)(bpy)(dfppe)][OTf]$_2$ (**14a** (85 %), **14b** (15 %)) (in acetone- d_6); (b) ^{31}P{^{1}H} NMR spectrum of isomeric aqua complexes (**14a**, **14b**); (c) IR spectrum of [Ru(H_2O)($P(OMe)_3$)(bpy)(dfppe)][OTf]$_2$ (**14a**, **14b**); (d) ^{13}C NMR spectrum of (**14a**, **14b**); (e) ES-MS spectrum of (**14a**, **14b**)

Figure S15. (a) ^{1}H NMR spectral stack plot (acetone-d_6, 293 K) for the reaction of [Ru(H_2O)($P(OMe)_3$)(bpy)(dfppe)][OTf]$_2$ (**14a**, **14b**) with H_2; (b) ^{31}P{^{1}H} NMR spectral stack plot (acetone-d_6, 293 K) for the reaction of (**14a**, **14b**) with H_2

Figure S16. ^{2}H NMR spectrum of [Ru(D)($P(OMe)_3$)(bpy)(dfppe)][OTf] (**11a-*d***) in acetone-d_6 at 293 K

Figure S17. (a) ^{1}H NMR spectrum of [Ru($NCCH_3$)($P(OMe)_3$)(bpy)(dfppe)][OTf]$_2$ (**15**); (b) ^{31}P{^{1}H} NMR spectrum of (**15**); (c) ^{13}C NMR spectrum of (**15**); (d) ES-MS spectrum of (**15)**

Table 2. Experimental elemental analysis data sheet along with a table for the compounds **11a**, **14**, **5**, **7**, **10**, **9**, **4**, **11c**, **8**.

Table 3. Experimental elemental analysis data sheet along with a table for the compounds **2**, **1**, **6**, **3**.

Table 4. Experimental elemental analysis data sheet along with a table for the compounds **6**, **9**.

Table 1. Crystallographic data for complexes **1, 2, 4, 6, 9, 10a** and **11c**

	1	**2**	**4**	**6**	**9**	**10a**	**11c**
Formula	$C_{34}H_{29}Cl_4F_{20}O_{4.50}P_2Ru_2S_4$	$C_{58}H_{22}Cl_5F_{40}O_3P_4Ru_2$	$C_{38.50}H_{18}Cl_2F_{20}N_2O_2P_2Ru$	$C_{43.50}H_{32}ClF_{23}N_2O_5P_3RuS$	$C_{68}H_{28}BClF_{44}N_2O_2P_2Ru$	$C_{42}H_{32}F_{23}N_2O_6P_3RuS$	$C_{40}H_{24}F_{23}N_2O_7P_3RuS$
Formula weight	1423.69	2030.03	1154.46	1361.20	1950.19	1323.74	1307.65
Crystal system	Triclinic	Triclinic	Monoclinic	Triclinic	Monoclinic	Monoclinic	Monoclinic
Space group	P-1	P-1	P21/c	P-1	C2/c	C2/c	C2/c
a (Å)	11.6961(5)	13.3638(10)	12.597(5)	16.2162(6)	45.7793(19)	35.246(5)	36.080(5)
b (Å)	15.1943(7)	15.3727(12)	11.179(5)	18.2514(7)	12.2606(6)	13.157(5)	12.8866(18)
c (Å)	15.9594(7)	18.2384(13)	28.426(5)	20.5416(7)	31.1479(14)	23.854(5)	24.761(4)
α(°)	96.611(2)	93.202(4)	90	109.4870(10)	90	90	90
β(°)	109.061(2)	110.568(4)	90.797	94.6870(10)	123.569(2)	117.195(10)	118.406(13)
γ(°)	111.884(2)	107.691(4)	90	113.2980(10)	90	90	90
V ($Å^{-3}$)	2395.11(18)	3286.1(4)	4003(2)	5101.3(3)	14567.0(11)	9839(4)	10127(3)
Z	2	2	4	4	8	8	8
D_{calc}(g/cm^{-3})	1.974	2.052	1.916	1.772	1.778	1.787	1.715
T (K)	110 (2)	100(2)	100(2)	100 (2)	100(2)	100(2)	110(2)
λ (Å)	0.71073	0.71073	0.71073	0.71073	0.71073	0.71073	0.71073
μ(mm^{-1})	1.213	0.922	0.740	0.626	0.457	0.595	0.579
R^a	0.0573	0.0490	0.0393	0.0453	0.0566	0.0727	0.0423
$R_w{}^a$	0.1359	0.1217	0.0861	0.1194	0.1613	0.2058	0.0942

[a] $R = \sum(|F_o| - |F_c|)/\sum|F_o|$, $R_w = [\sum w(|F_o| - |F_c|)^2/\sum w|F_o|^2]^{1/2}$ (based on reflections with $I > 2\sigma(I)$)

Figure S1. (a) ORTEP view of [(dfppe)ClRu(μ-Cl)$_3$Ru(dmso-S)$_3$] complex (**1**) and selected bond lengths and bond angles

ORTEP view of the complex [(dfppe)ClRu(μ-Cl)$_3$Ru(dmso-S)$_3$] (**1**) showing the atom labeling and 50% probability ellipsoids (Hydrogen atoms and solvent are omitted for clarity). Bond lengths (Å): Ru(1)-P(2) 2.2144(15), Ru(1)-P(1) 2.2369(14), Ru(1)-Cl(4) 2.3653(13), Ru(1)-Cl(2) 2.4227(14), Ru(1)-Cl(3) 2.4840(14), Ru(1)-Cl(1) 2.4990(12), Ru(2)-S(2) 2.2672(15), Ru(2)-S(3) 2.2659(13), Ru(2)-S(1) 2.2705(14), Ru(2)-Cl(1) 2.4227(13), Ru(2)-Cl(2) 2.4245(13), Ru(2)-Cl(3) 2.4526(12); Bond angles (deg): P(2)-Ru(1)-P(1) 83.87(5), Ru(2)-Cl(1)-Ru(1) 82.02(4), Ru(1)-Cl(2)-Ru(2) 83.57(4), Ru(2)-Cl(3)-Ru(1) 81.73(4).

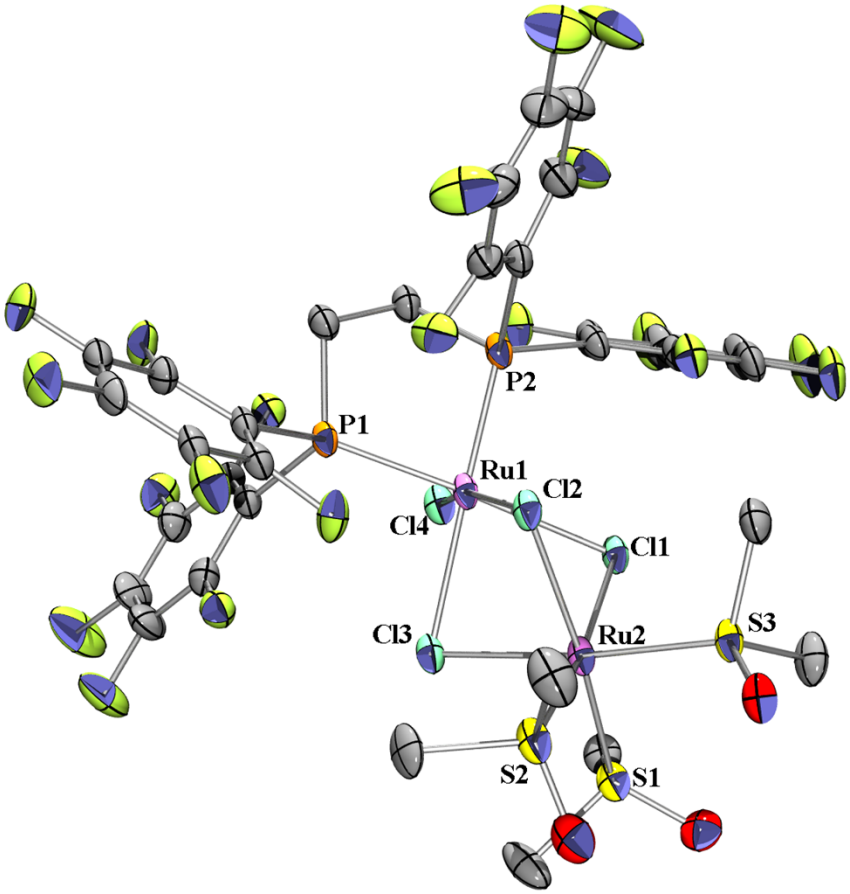

(b) ^{1}H NMR spectrum of [(dfppe)ClRu(μ-Cl)$_3$Ru(dmso-S)$_3$] (**1**)

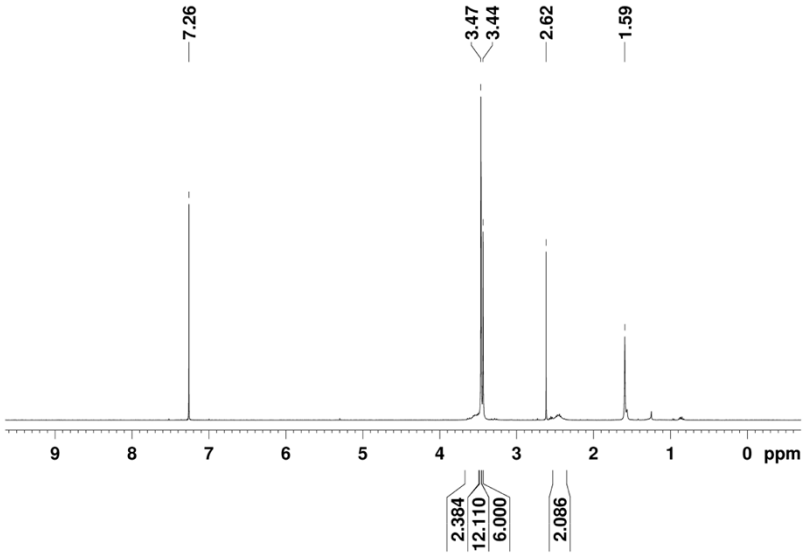

(c) $^{31}P\{^{1}H\}$ NMR spectrum of [(dfppe)ClRu(μ-Cl)$_3$Ru(dmso-S)$_3$] (**1**)

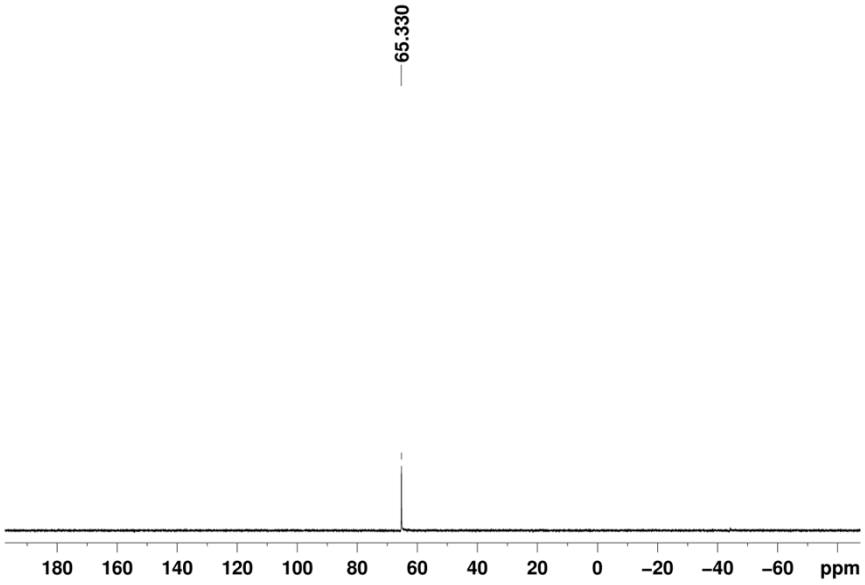

(d)^{19}F NMR spectrum of [(dfppe)ClRu(μ-Cl)$_3$Ru(dmso-S)$_3$] (**1**)

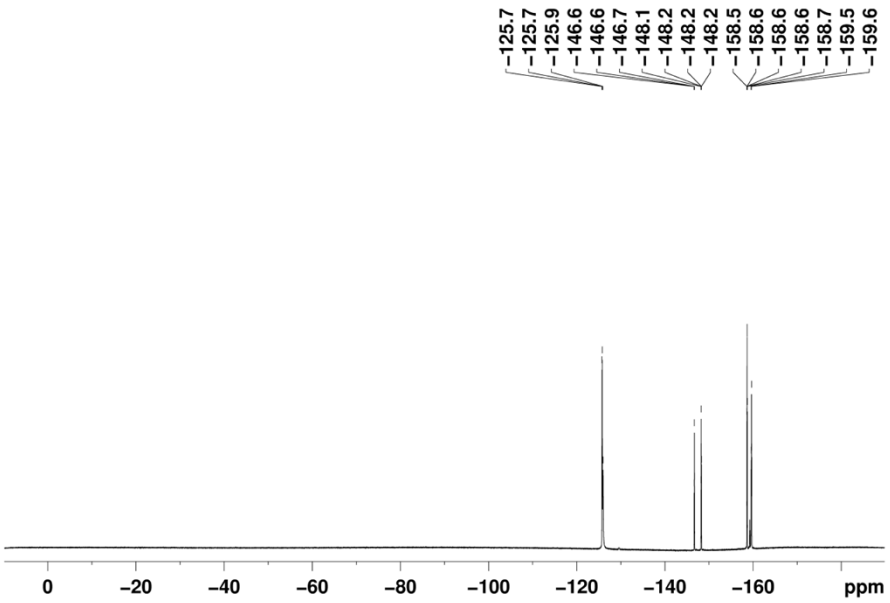

(e) ^{13}C NMR spectrum of [(dfppe)ClRu(μ-Cl)$_3$Ru(dmso-S)$_3$] (**1**)

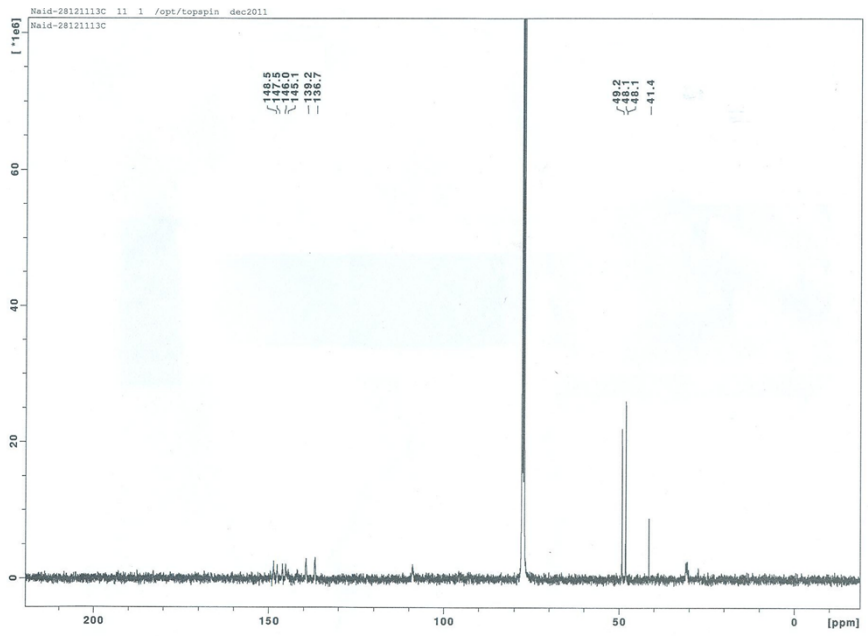

Figure S2. (a**)** ORTEP view of [(dfppe)ClRu(μ-Cl)$_3$Ru(dfppe)Cl] complex (**2**) and selected bond lengths and bond angles

ORTEP view of the complex [(dfppe)ClRu(μ-Cl)$_3$Ru(dfppe)Cl] (**2**) showing the atom labeling and 50% probability ellipsoids (Hydrogen atoms and solvent are omitted for clarity). Bond lengths (Å): Ru(1)-P(1) 2.2399(11), Ru(1)-P(2) 2.2434(10), Ru(1)-Cl(3) 2.3902(11), Ru(1)-Cl(1) 2.4182(11), Ru(1)-Cl(4) 2.4899(10), Ru(1)-Cl(2) 2.4970(10), Ru(2)-P(4) 2.2067(11), Ru(2)-P(3) 2.2580(11), Ru(2)-Cl(5) 2.4174(10), Ru(2)-Cl(2) 2.4970(10), Ru(2)-Cl(4) 2.4950(10); Bond angles (deg): P(1)-Ru(1)-P(2) 85.33(4), P(4)-Ru(2)-P(3) 83.81(4), Ru(2)-Cl(2)-Ru(1) 82.43(3), Ru(2)-Cl(3)-Ru(1) 86.39(3), Ru(1)-Cl(4)-Ru(2) 82.03(3).

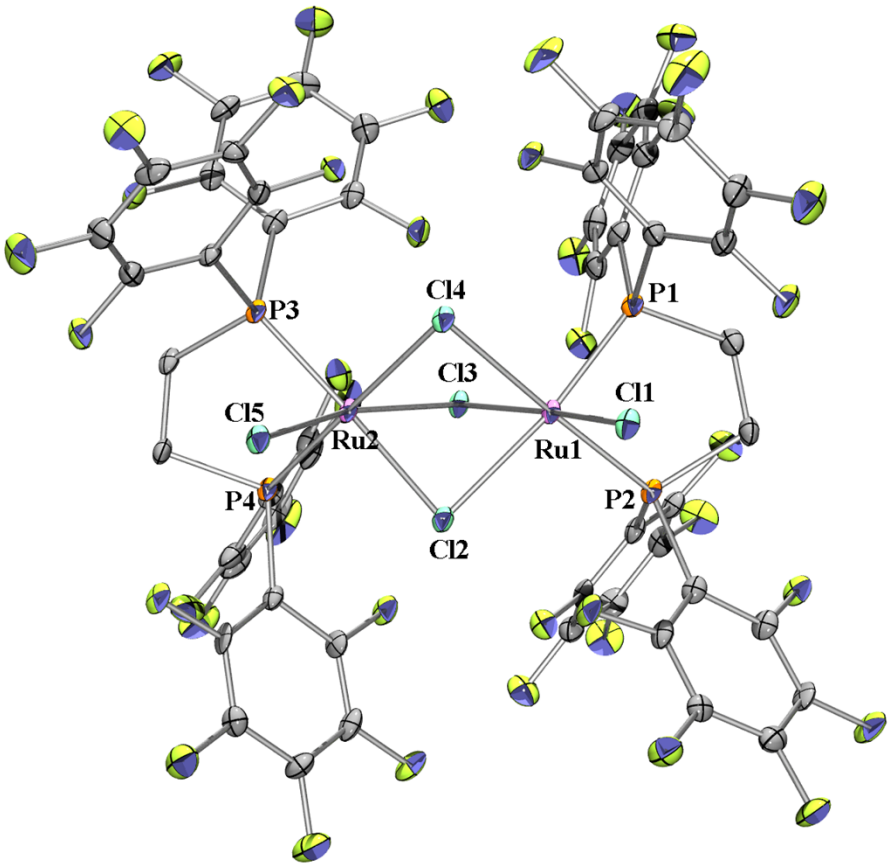

(b) ^{1}H NMR spectrum of [(dfppe)ClRu(μ-Cl)$_3$RuCl(dfppe)] (**2**)

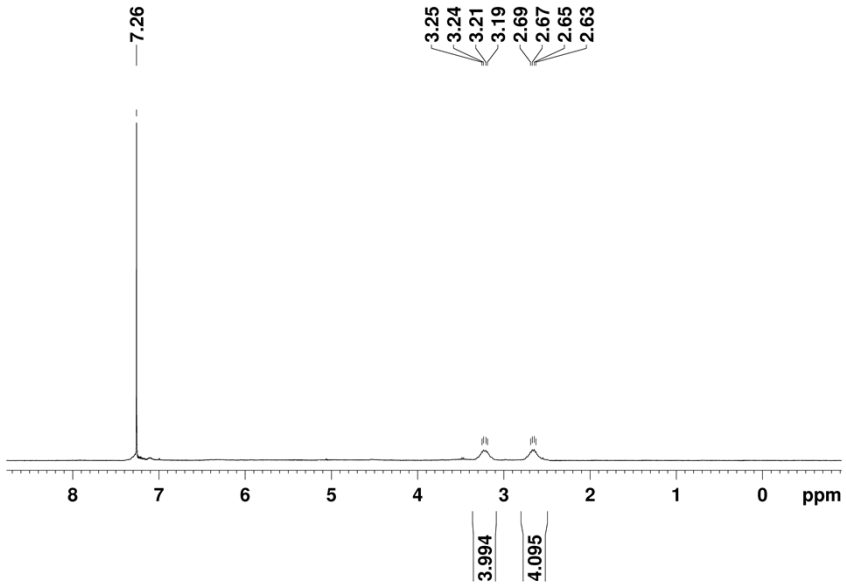

(c) ^{31}P NMR spectrum of [(dfppe)ClRu(μ-Cl)$_3$RuCl(dfppe)] (**2**)

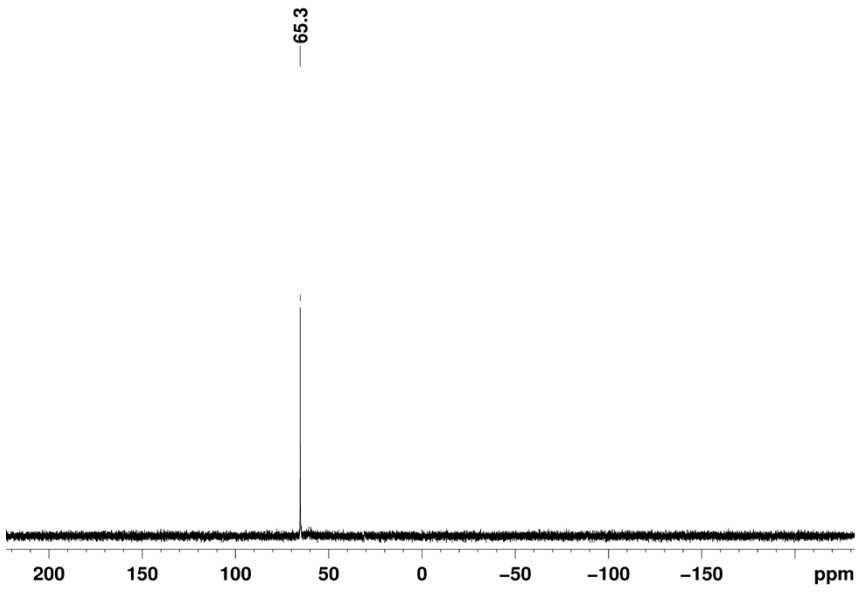

Figure S3. (a) ^{1}H NMR spectrum of *trans*-[$RuCl_2$(bpy)(dfppe)] (**3**)

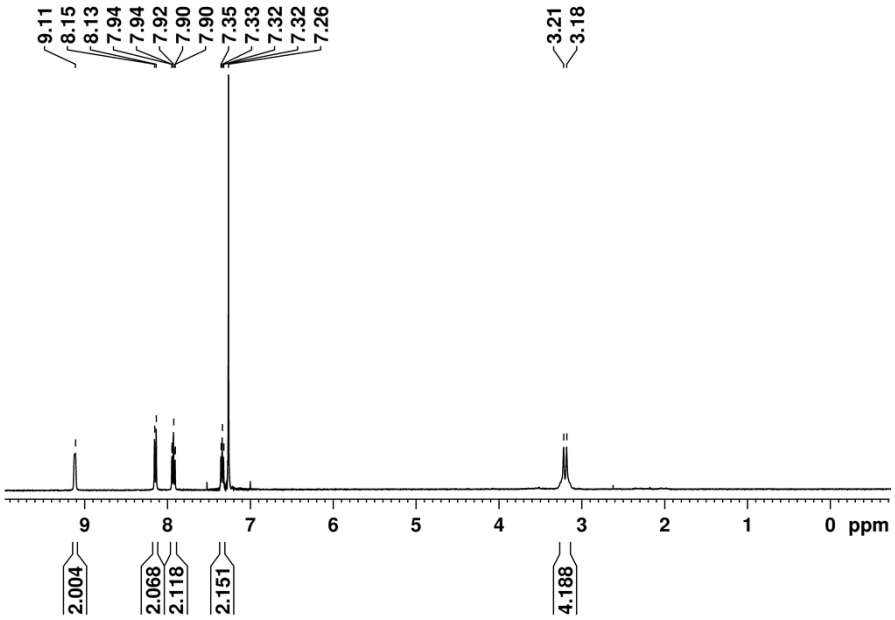

(b) ^{31}P NMR spectrum of *trans*-[$RuCl_2$(bpy)(dfppe)] (**3**)

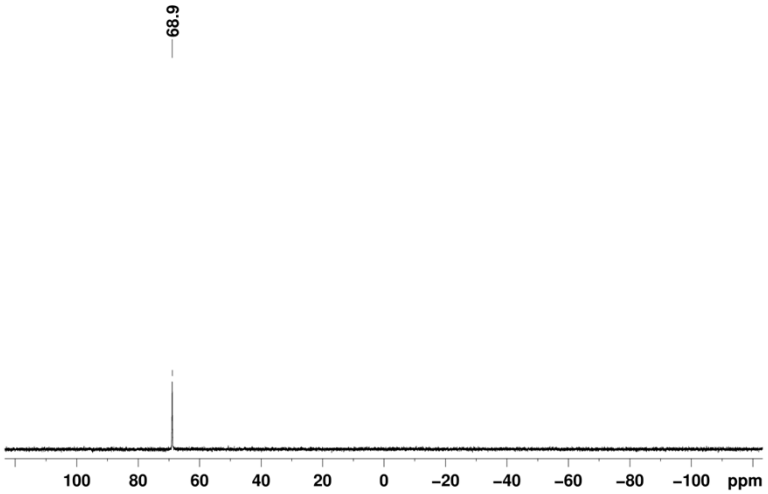

(c) ^{19}F NMR spectrum of *trans*-[$RuCl_2$(bpy)(dfppe)] (**3**)

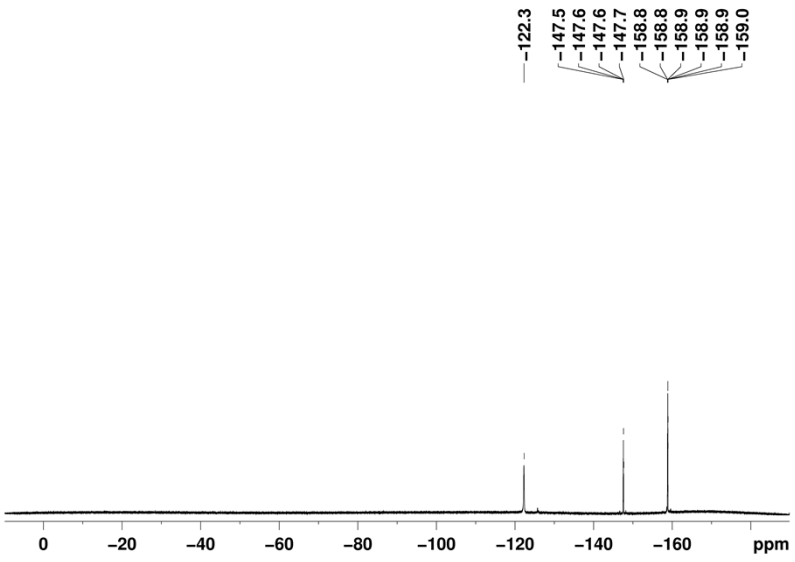

(d) ^{13}C NMR spectrum of *trans*-[$RuCl_2$(bpy)(dfppe)] (**3**)

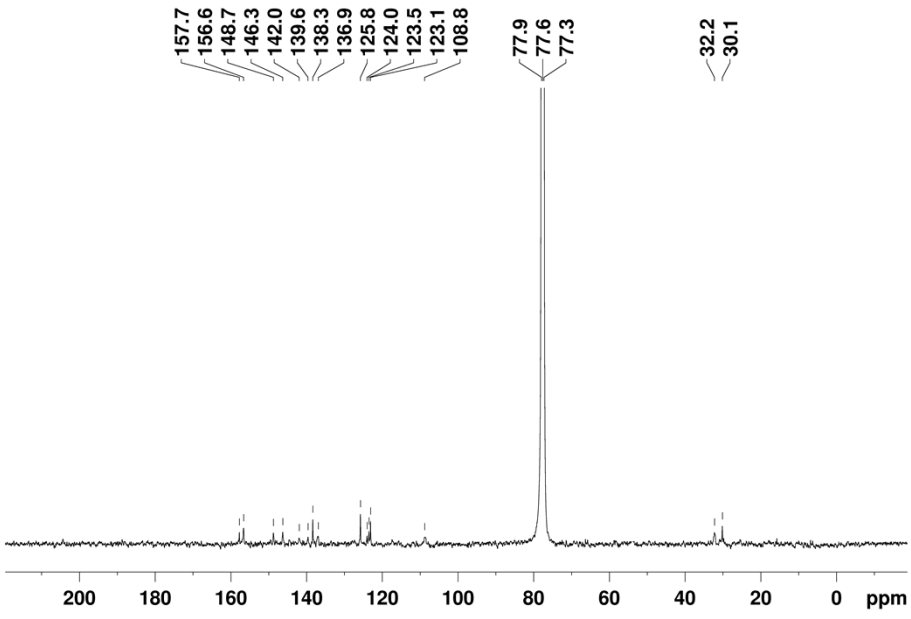

(e) ES-MS spectrum of the complex *trans*-[$RuCl_2$(bpy)(dfppe)] (**3**)

Calculated Mass spectrum (**3**)

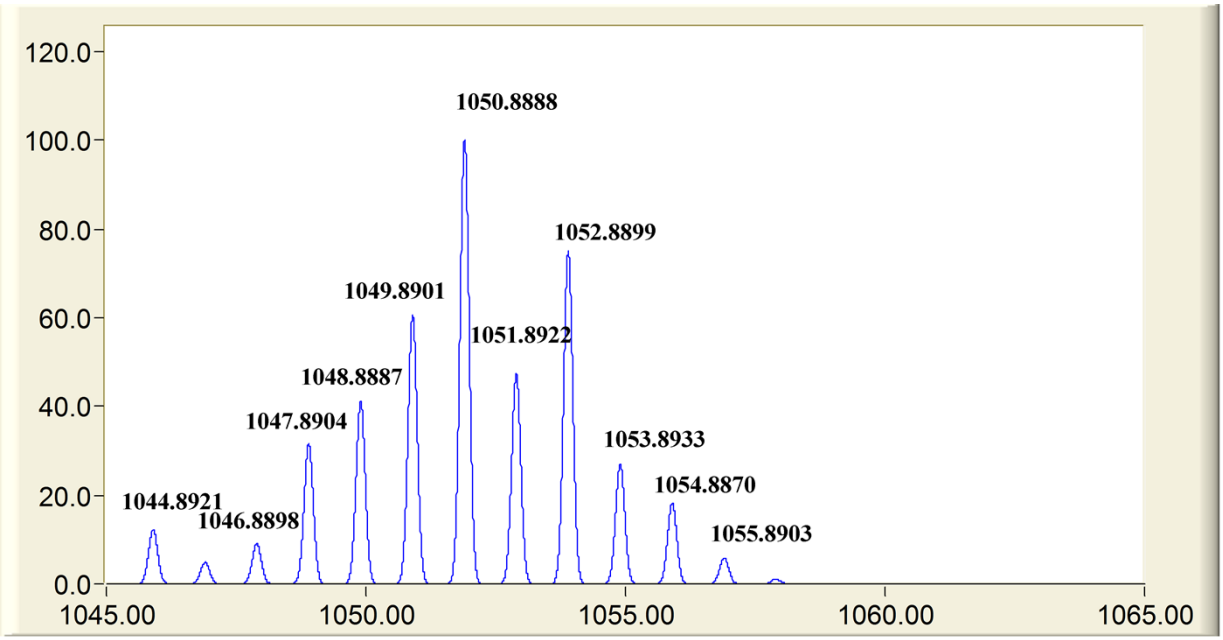

Experimental Mass spectrum of (**3**): m/z = 1050. 9102 [$M^+ - Cl^-$]

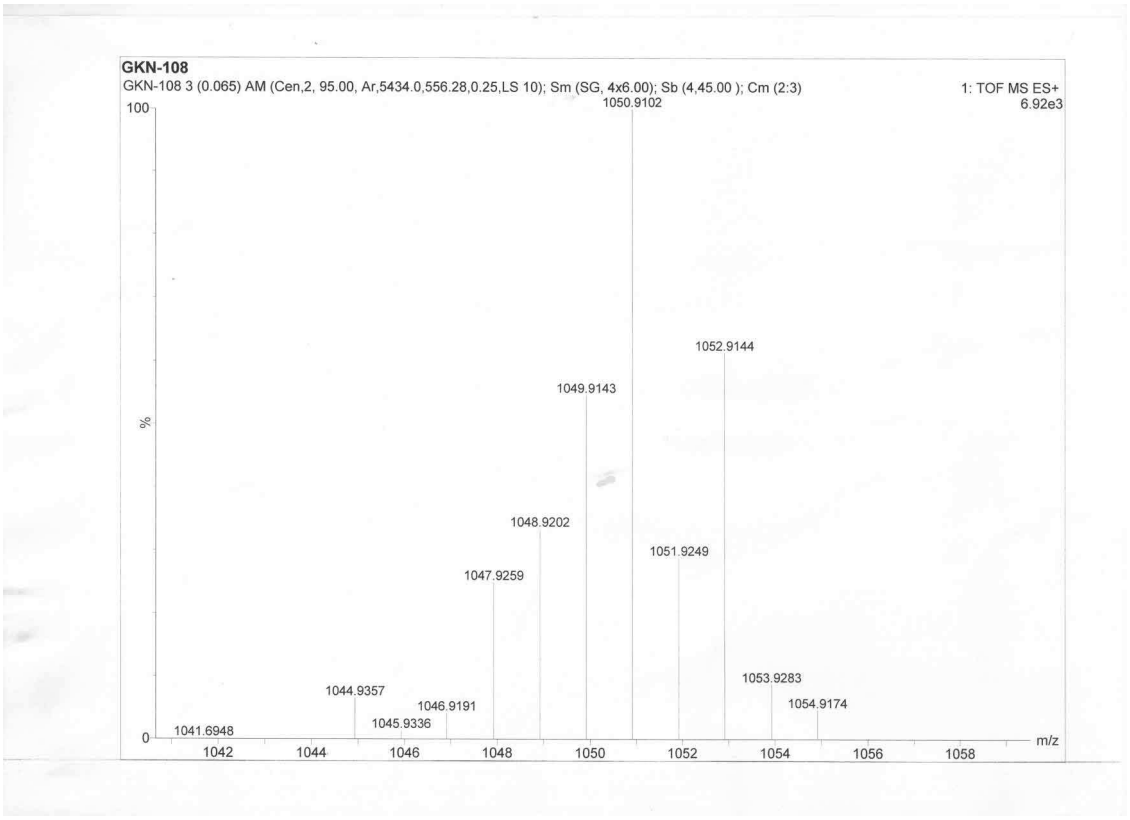

Figure S4. (a**)** ORTEP view of *trans*-[$RuCl_2$(phen)(dfppe)] complex (**4**) and selected bond lengths and bond angles

ORTEP view of the complex *trans*-[$RuCl_2$(Phen)(dfppe)] (**4**) showing the atom labeling and 50% probability ellipsoids (Hydrogen atoms and solvent are omitted for clarity). Bond lengths (Å): Ru(1)-N(1) 2.130(3), Ru(1)-N(2) 2.131(3), Ru(1)-P(2) 2.2763(11), Ru(1)-P(1) 2.2932(10), Ru(1)-Cl(1) 2.3945(9), Ru(1)-Cl(2) 2.3973(9) Bond angles(deg): N(1)-Ru(1)-N(2) 77.78(10), N(1)-Ru(1)-P(2) 176.79(8), N(2)-Ru(1)-P(2) 99.03(8), N(1)-Ru(1)-P(1) 99.27(8), N(2)-Ru(1)-P(1) 175.93(8), P(2)-Ru(1)-P(1) 83.93(4)

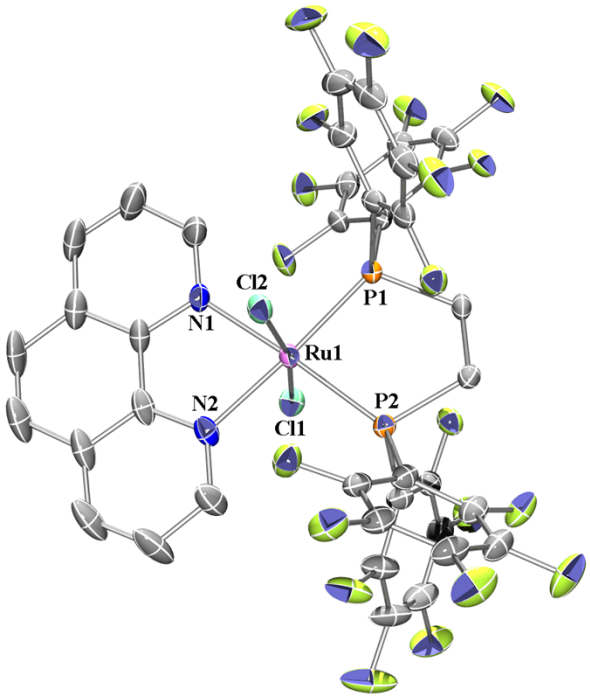

(b) ^{1}H NMR spectrum of *trans*-[$RuCl_2$(phen)(dfppe)] (**4**)

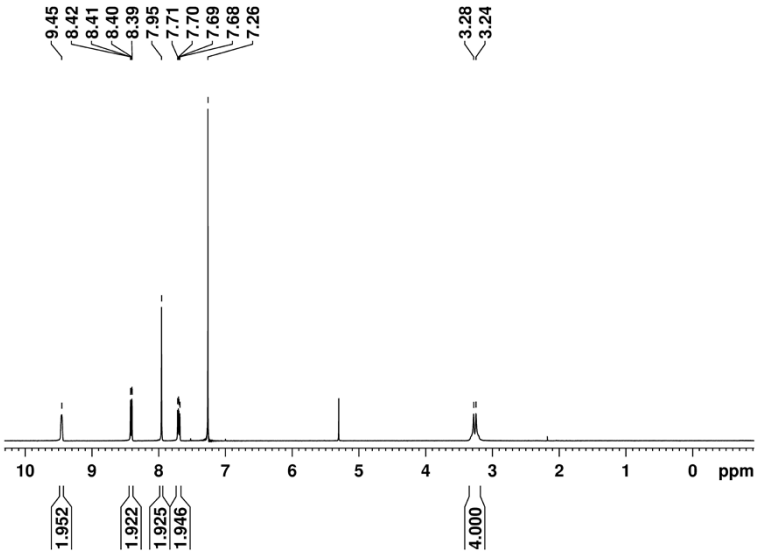

(c) ^{31}P NMR spectrum of *trans*-[$RuCl_2$(phen)(dfppe)] (**4**)

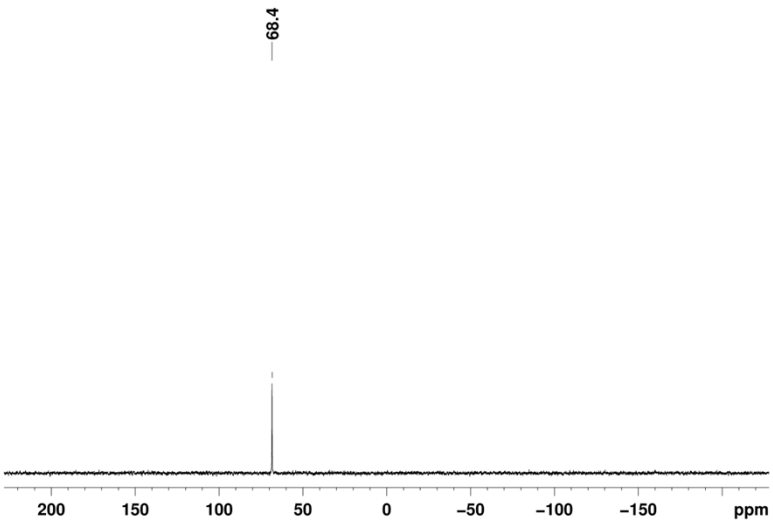

(d) ^{19}F NMR spectrum of *trans*-[$RuCl_2$(phen)(dfppe)] (**4**)

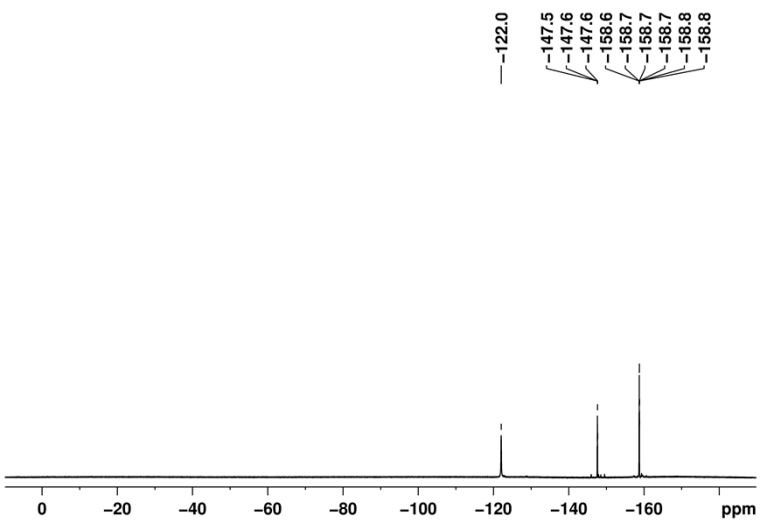

(e) ^{13}C NMR spectrum of *trans*-[$RuCl_2$(phen)(dfppe)] (**4**)

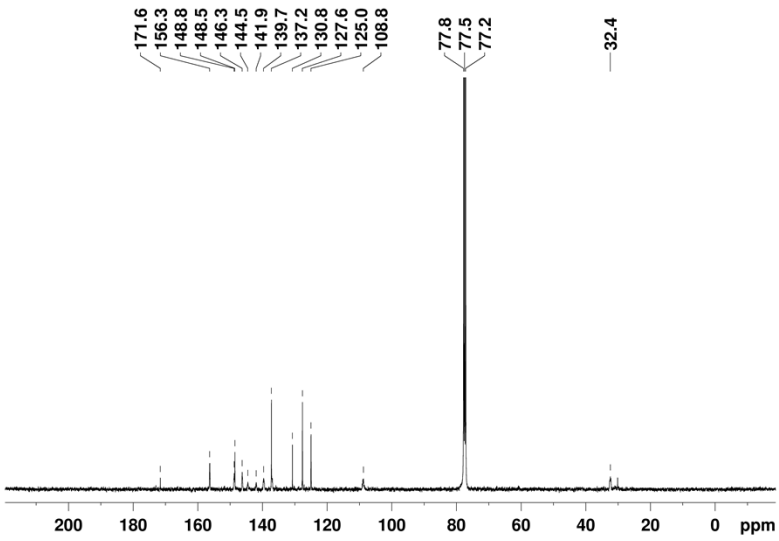

(f) ES-MS spectrum of *trans*-[$RuCl_2$(phen)(dfppe)] (**4**)

Calculated Mass spectrum of (**4**)

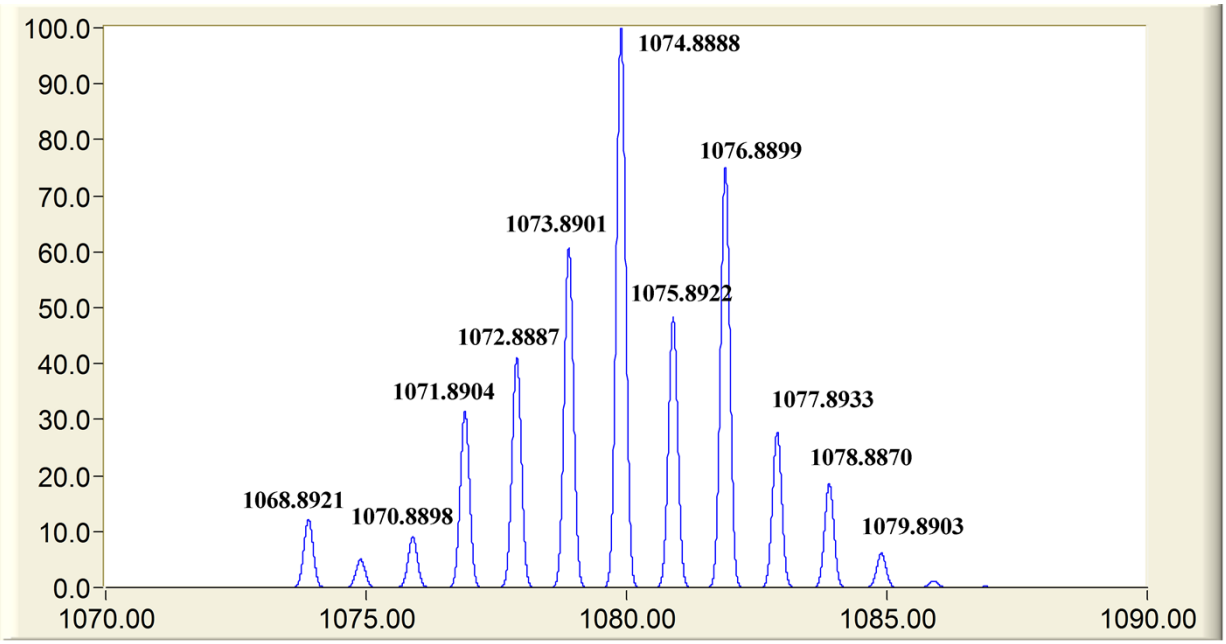

Experimental Mass spectrum of (**4**): m/z = 1074.9425 [$M^+ - Cl^-$]

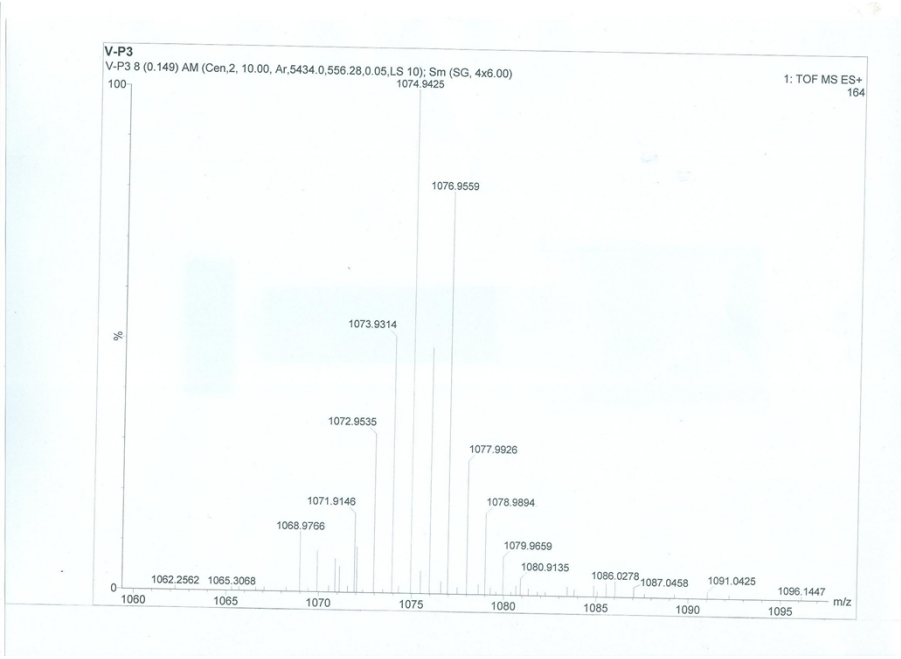

Figure S5. (a) ^{1}H NMR spectrum of $[RuCl(P(OMe)_3)(bpy)(dfppe)]^+$ (**5**)

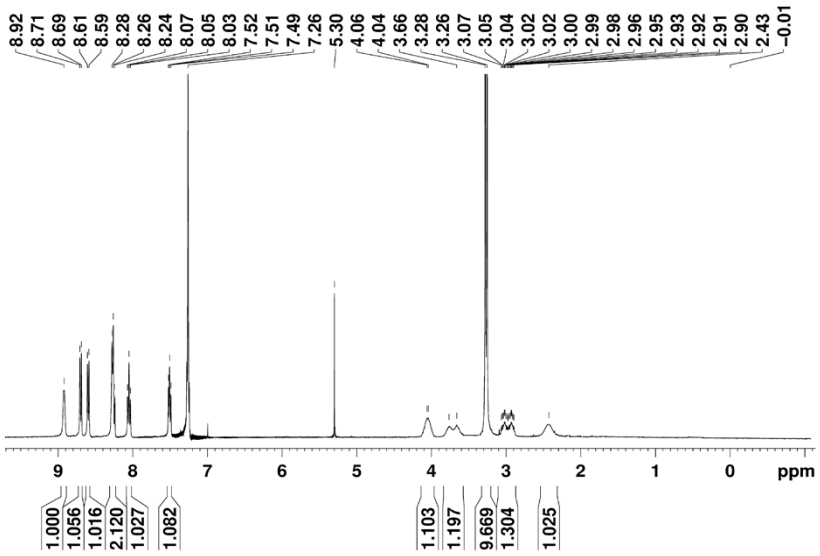

(b) ^{31}P NMR spectrum of $[RuCl(P(OMe)_3)(bpy)(dfppe)]^+$ (**5**)

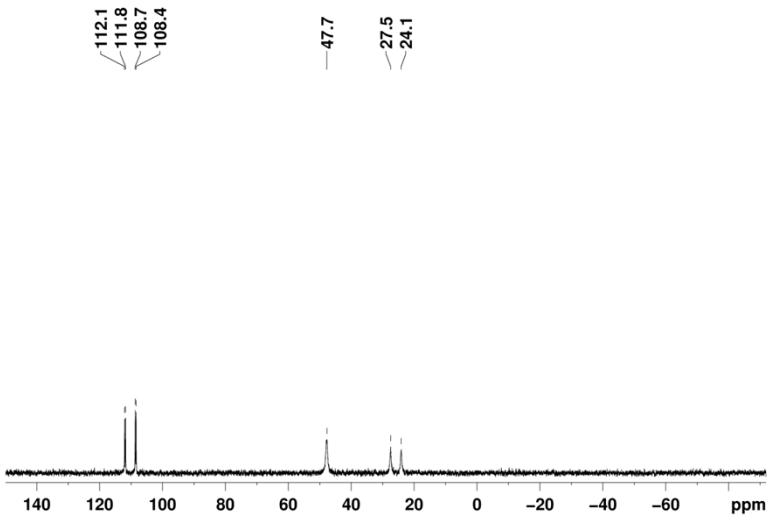

(c) ^{19}F NMR spectrum of $[RuCl(P(OMe)_3)(bpy)(dfppe)]^+$ (**5**)

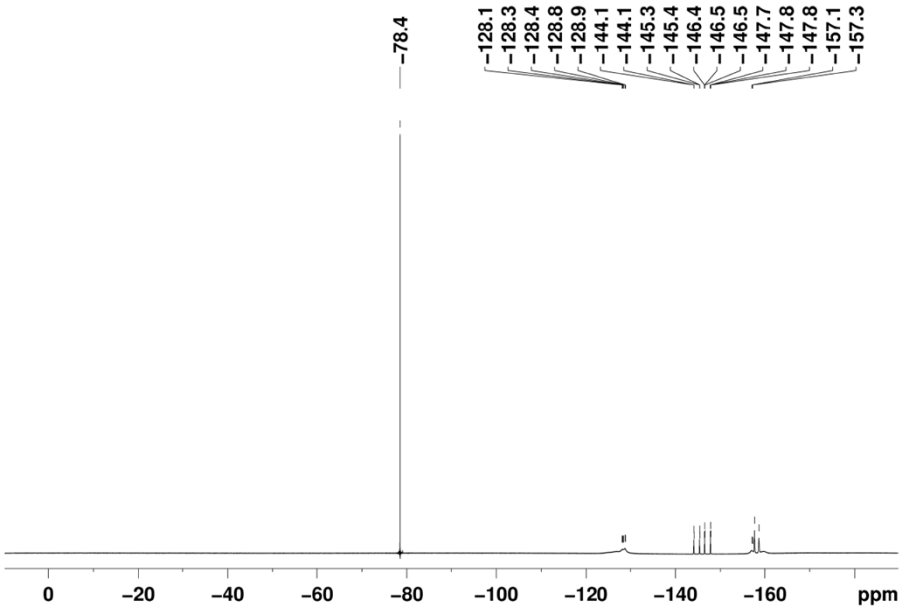

(d) ^{13}C NMR spectrum of $[RuCl(P(OMe)_3)(bpy)(dfppe)]^+$ (**5**)

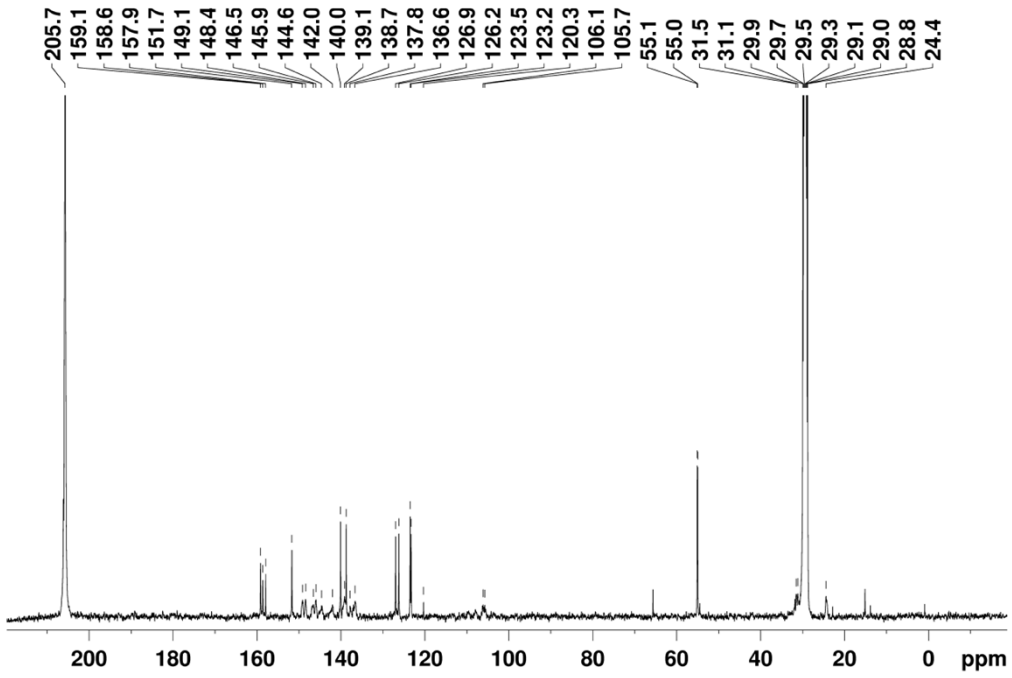

(e) ES-MS spectrum of $[RuCl(P(OMe)_3)(bpy)(dfppe)]^+$ (**5**)

Calculated Mass spectrum of (**5**)

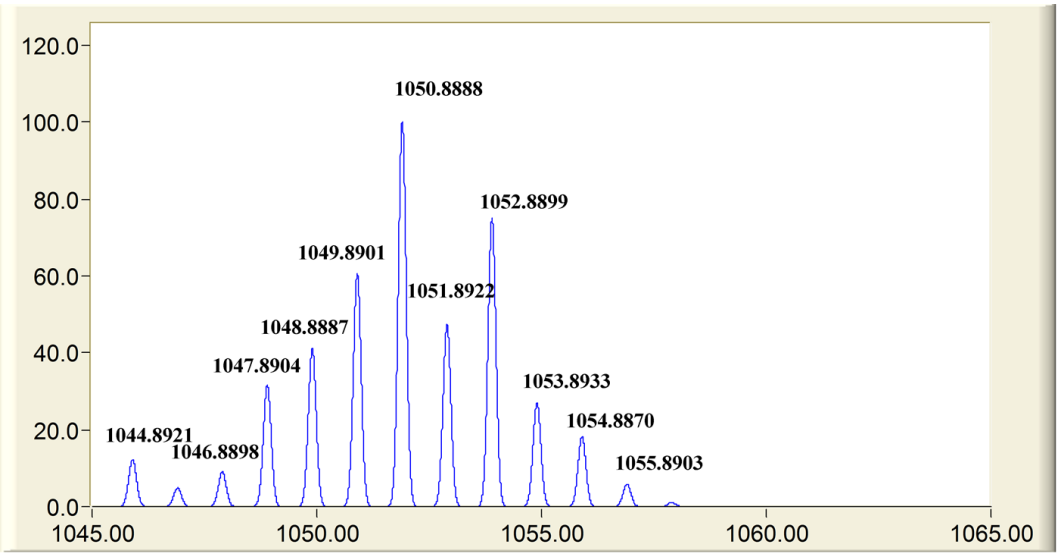

Experimental Mass spectrum of (**5**) m/z = 1050.8887 $[M^+ - (P(OMe)_3+OTf^-)]$

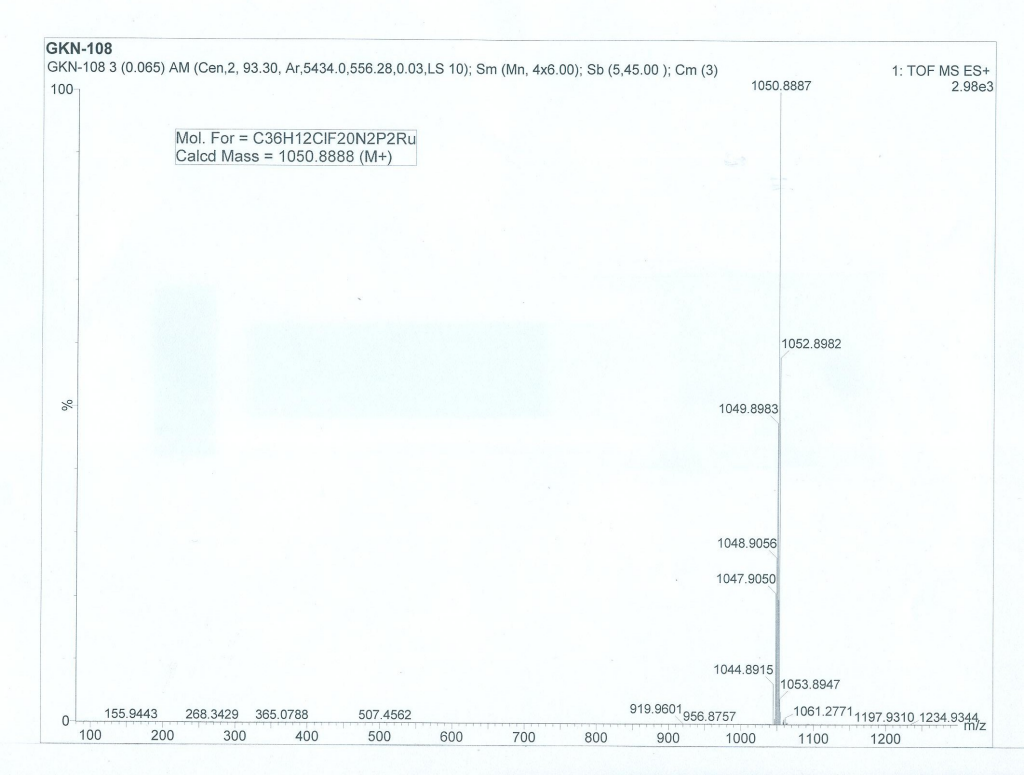

Figure S6. (a) ORTEP view of [RuCl(PMe_3)(bpy)(dfppe)] cation (**6**) and selected bond lengths and bond angles

ORTEP view of the [RuCl(PMe_3)(bpy)(dfppe)] (**6**) cation at the 50% probability level. Solvent, disorder, and all hydrogen atoms are omitted for clarity. There are two independent molecules in the asymmetric unit; only one molecule is shown. Selected bond lengths (Å): Ru(1)-N(1) 2.073(3), Ru(1)-N(2) 2.102(3), Ru(1)-P(1) 2.2938(8), Ru(1)-P(3) 2.3747(11), Ru(1)-P(2) 2.4103(10), Ru(1)-Cl(1) 2.4233(9); Bond angles(deg): N(1)-Ru(1)-N(2) 78.16(12), N(1)-Ru(1)-P(1) 104.44(9), N(2)-Ru(1)-P(1) 171.87(10), N(1)-Ru(1)-P(3) 85.33(9), N(2)-Ru(1)-P(3) 87.90(10), P(1)-Ru(1)-P(3) 99.94(3), N(1)-Ru(1)-P(2) 105.93(9), N(2)-Ru(1)-P(2) 91.02(10), P(1)-Ru(1)-P(2) 80.86(3), P(3)-Ru(1)-P(2) 168.22(4)

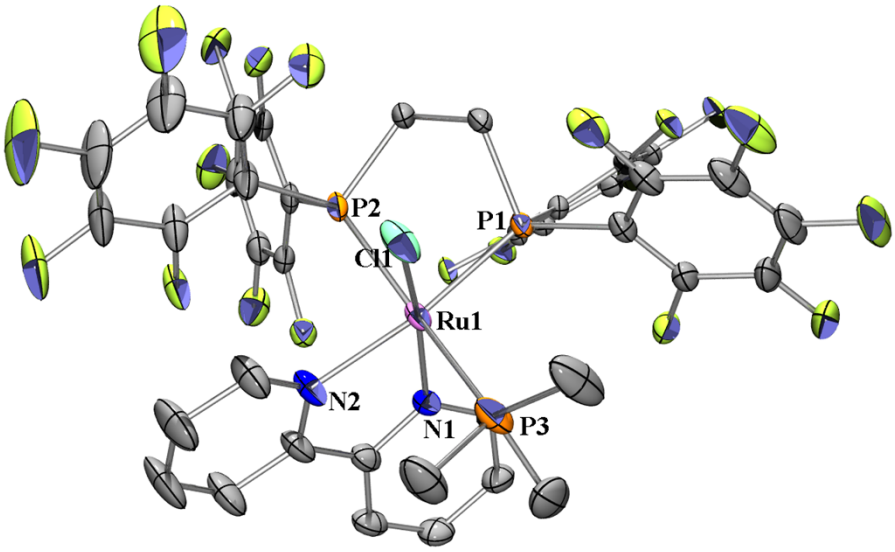

(b) ^{1}H NMR spectrum of $[RuCl(PMe_3)(bpy)(dfppe)]^{+}$ (**6**)

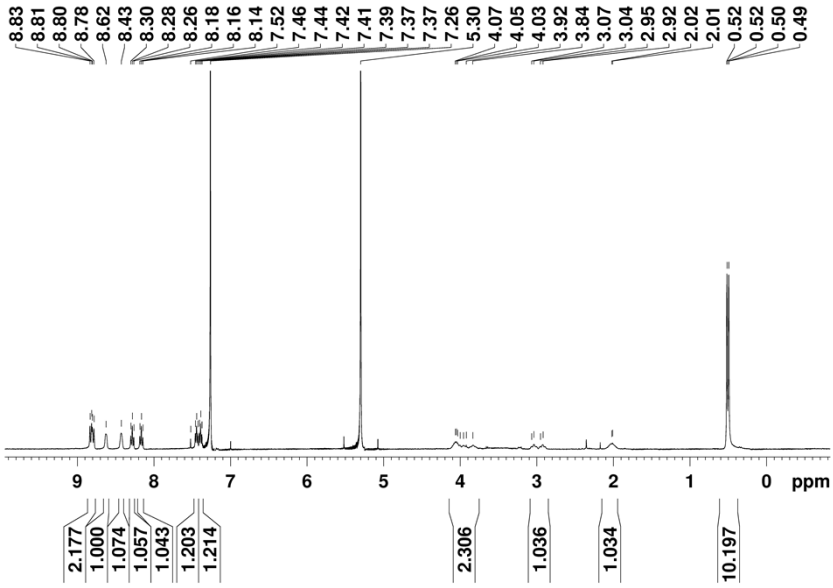

(c) ^{31}P NMR spectrum of $[RuCl(PMe_3)(bpy)(dfppe)]^{+}$ (**6**)

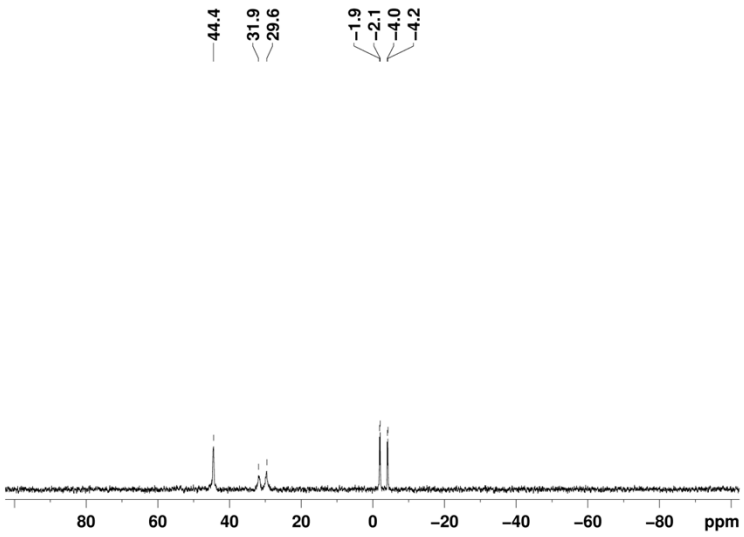

(d) ^{19}F NMR spectrum of $[RuCl(PMe_3)(bpy)(dfppe)]^+$ (**6**)

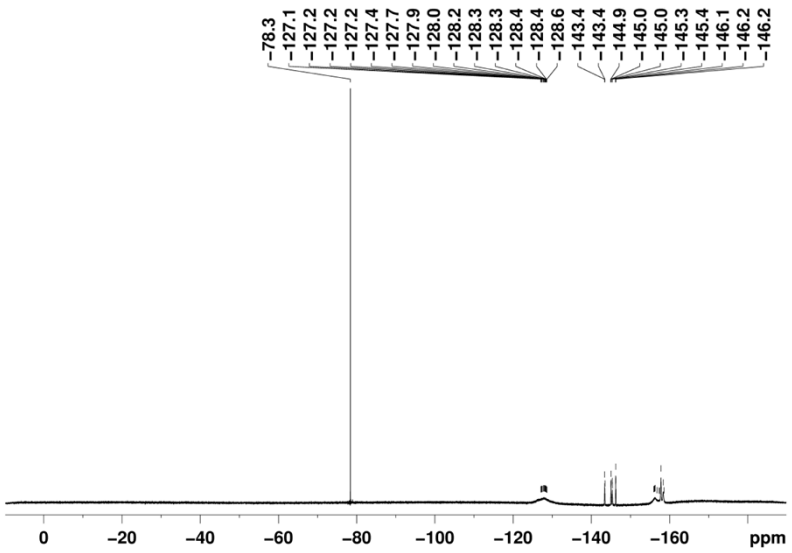

(e) ^{13}C NMR spectrum of $[RuCl(PMe_3)(bpy)(dfppe)]^+$ (**6**)

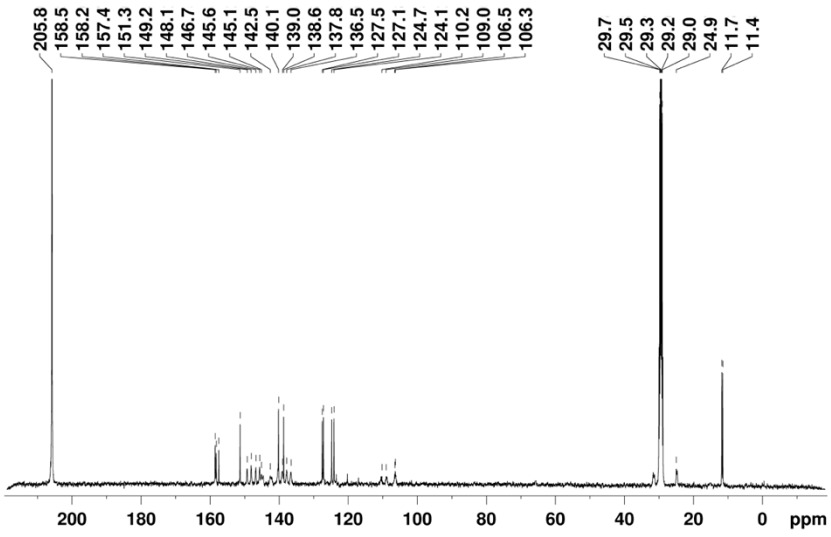

(f) ES-MS spectrum of $[RuCl(PMe_3)(bpy)(dfppe)]^+$ (**6**)

Calculated Mass spectrum of (**6**)

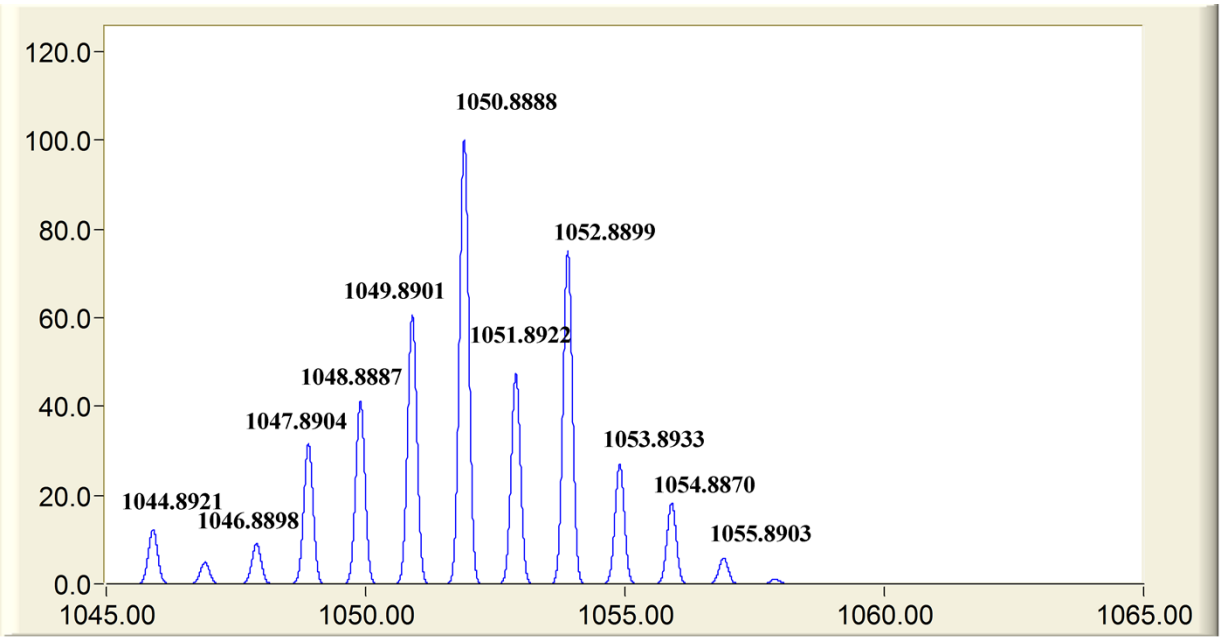

Experimental Mass spectrum of (**6**)

m/z = 1050.8882 $[M^+ - (PMe_3+OTf^-)]$

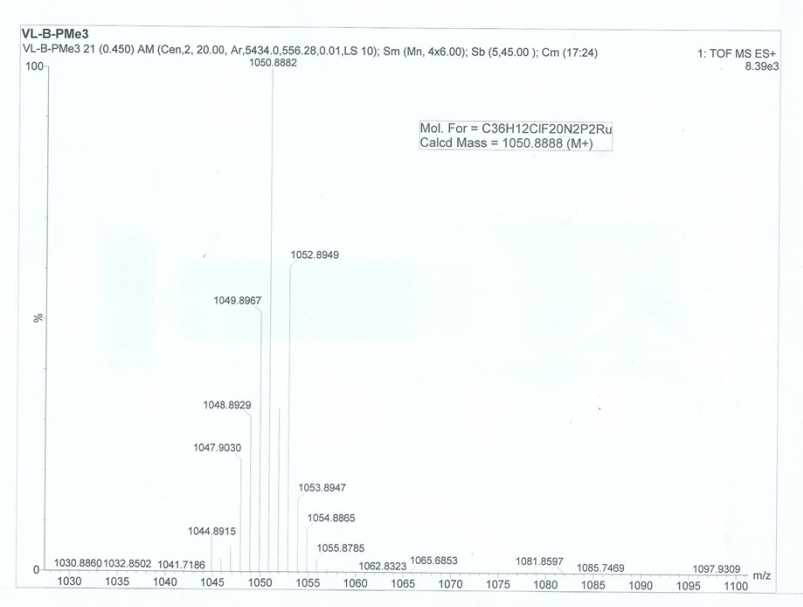

Figure S7. (a) ^{1}H NMR spectrum of $[RuCl(NCCH_3)(bpy)(dfppe)]^{+}$ (**7**)

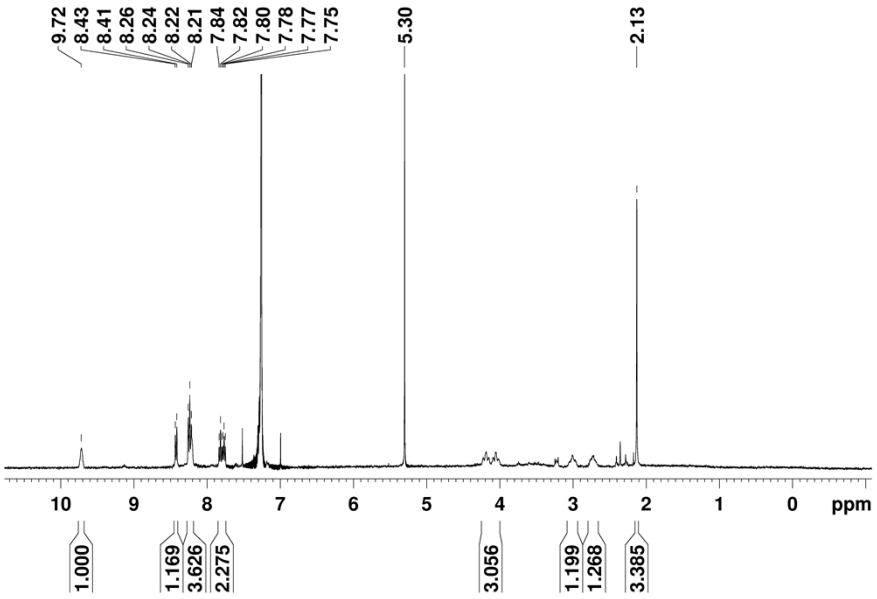

(b) ^{31}P NMR spectrum of $[RuCl(NCCH_3)(bpy)(dfppe)]^{+}$ (**7**)

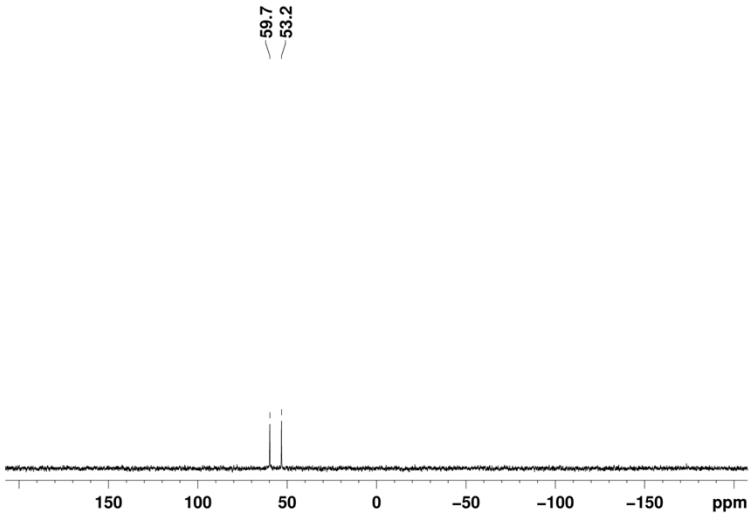

(c) ^{19}F NMR spectrum of $[RuCl(NCCH_3)(bpy)(dfppe)]^+$ (**7**)

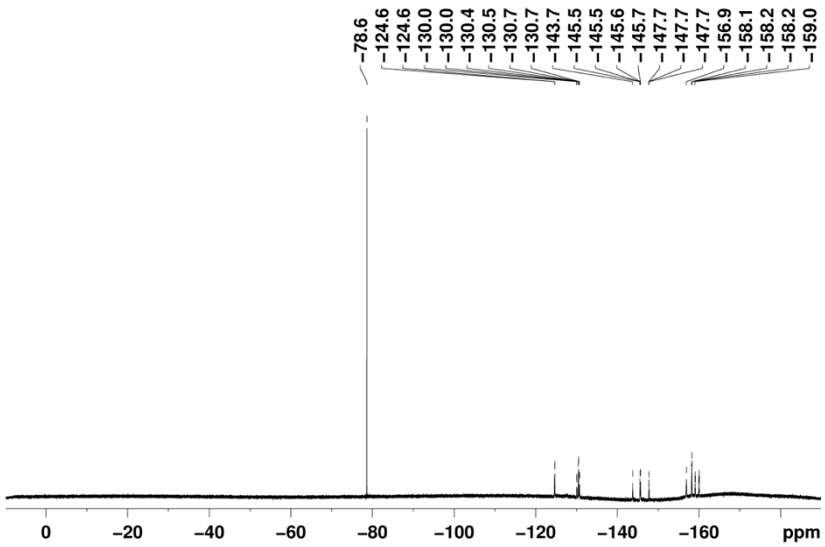

(d) ES-MS spectrum of the complex $[RuCl(NCCH_3)(bpy)(dfppe)][OTf]$ (**7**)

Calculated Mass spectrum of (**7**)

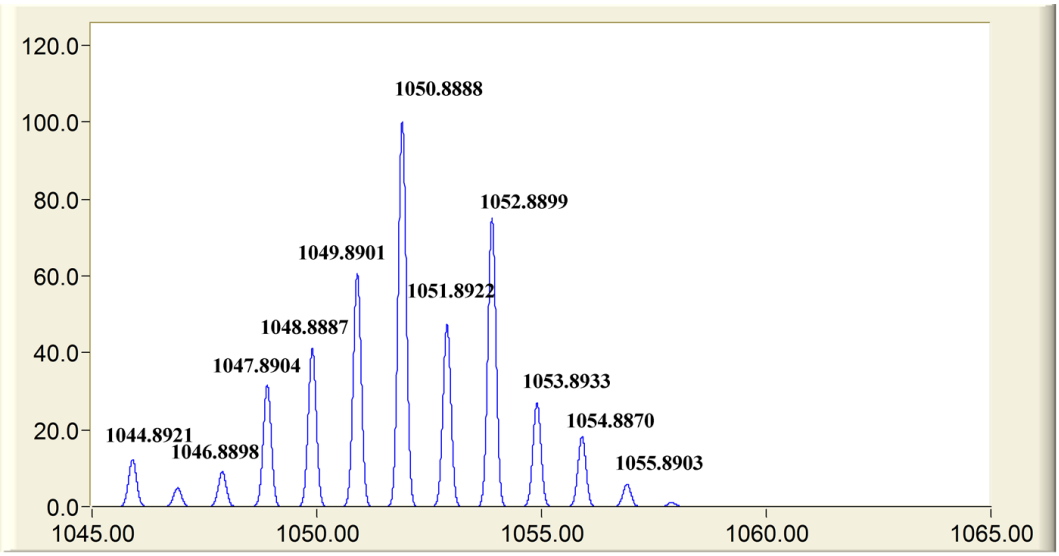

Experimental spectrum of (**7**)

m/z = 1050.8889 [M^+ - (CH_3CN + OTf^-)]

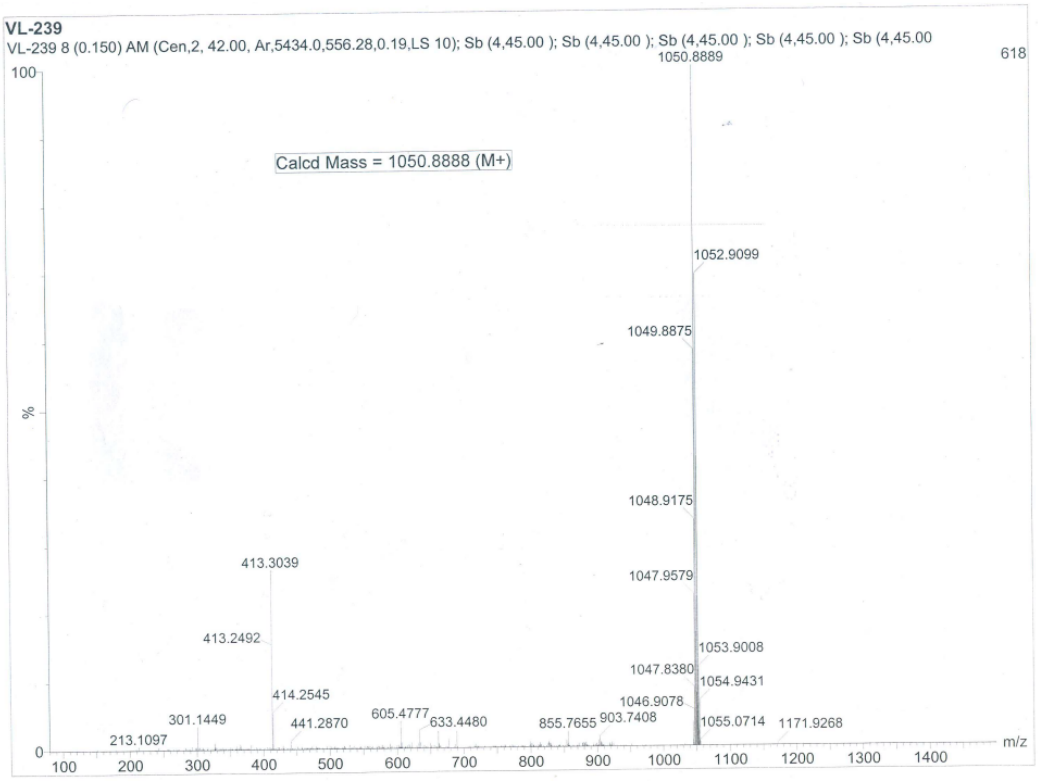

Figure S8. (a) ^{1}H NMR spectrum of [RuCl(CO)(bpy)(dfppe)]$^{+}$ (**8**)

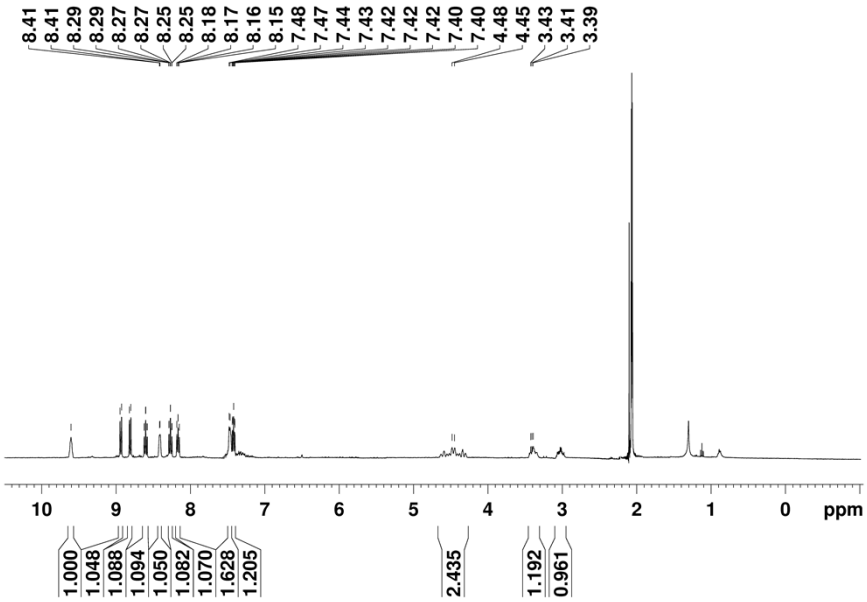

(b) ^{31}P NMR spectrum of [RuCl(CO)(bpy)(dfppe)]$^{+}$ (**8**)

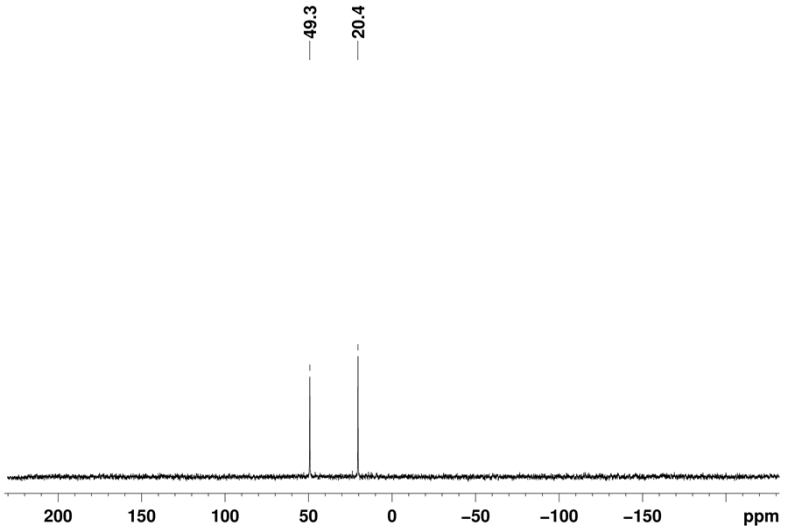

(c) ^{13}C NMR spectrum of $[RuCl(CO)(bpy)(dfppe)]^+$ (**8**)

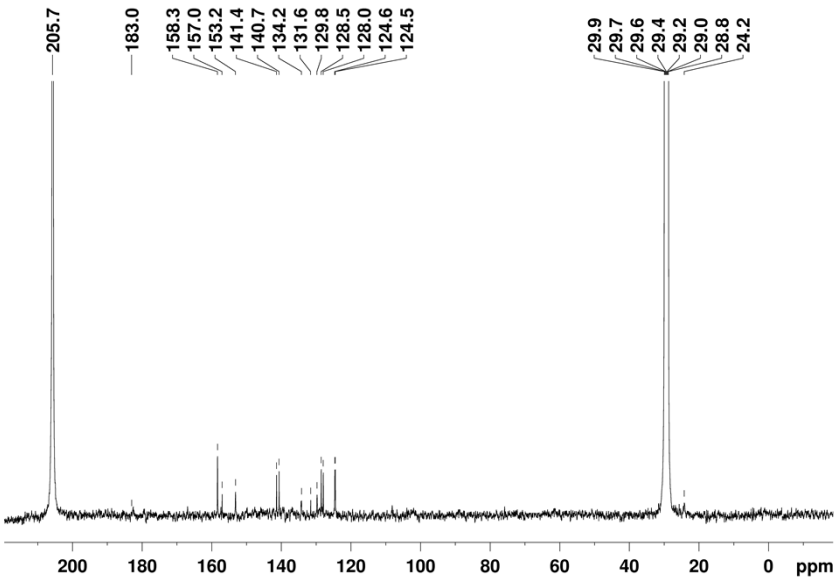

(d) IR spectrum of [RuCl(CO)(bipy)(dfppe)][OTf], [ν (CO)] = 2040 cm^{-1}

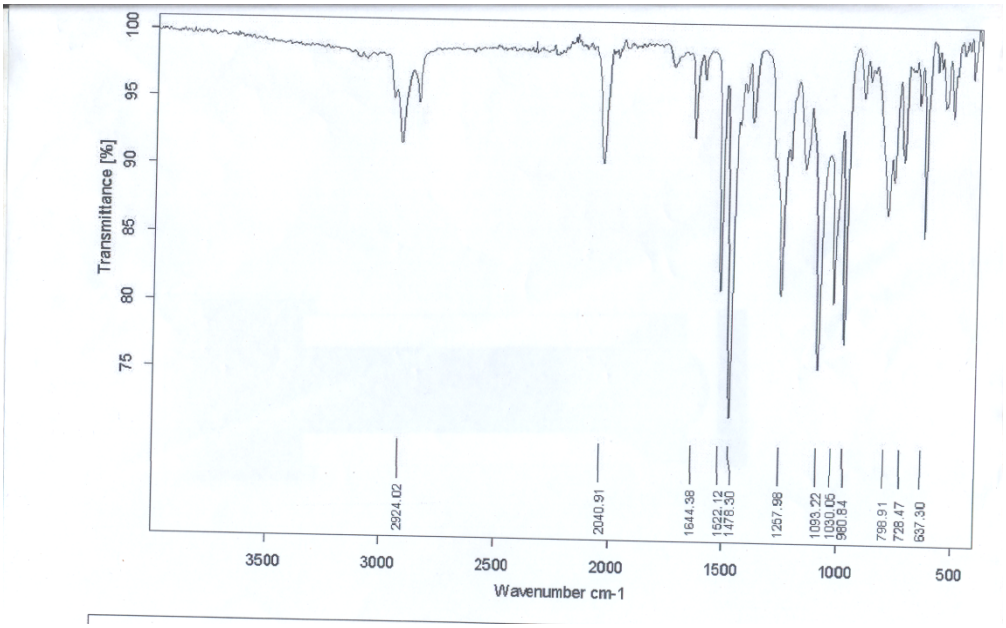

(e) ES-MS spectrum of $[RuCl(CO)(bpy)(dfppe)]^+$ (**8**)

Calculated Mass spectrum

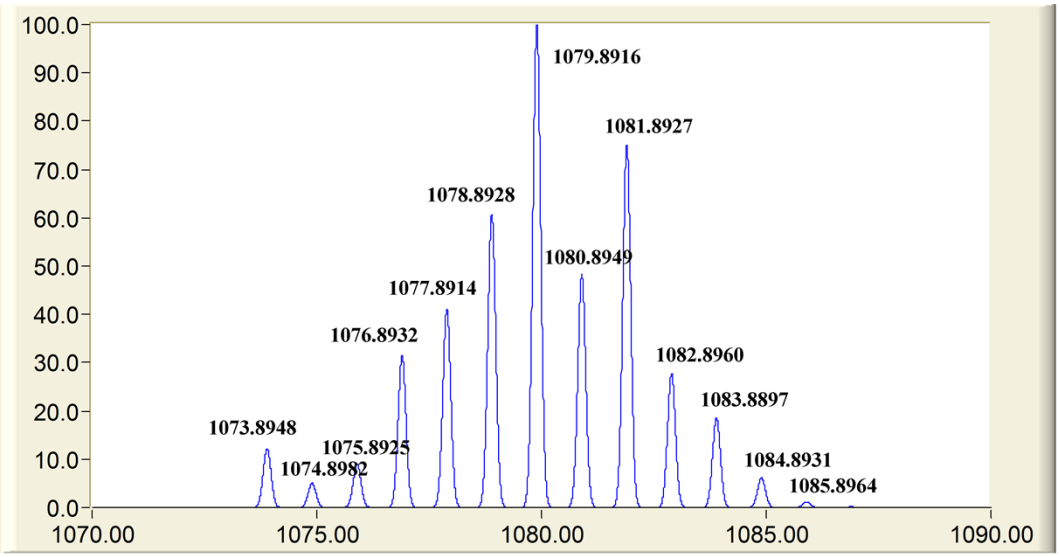

Experimental Mass Spectrum

m/z = 1079.1661 $[(M+H)^+ - (CO + OTf^-)]$

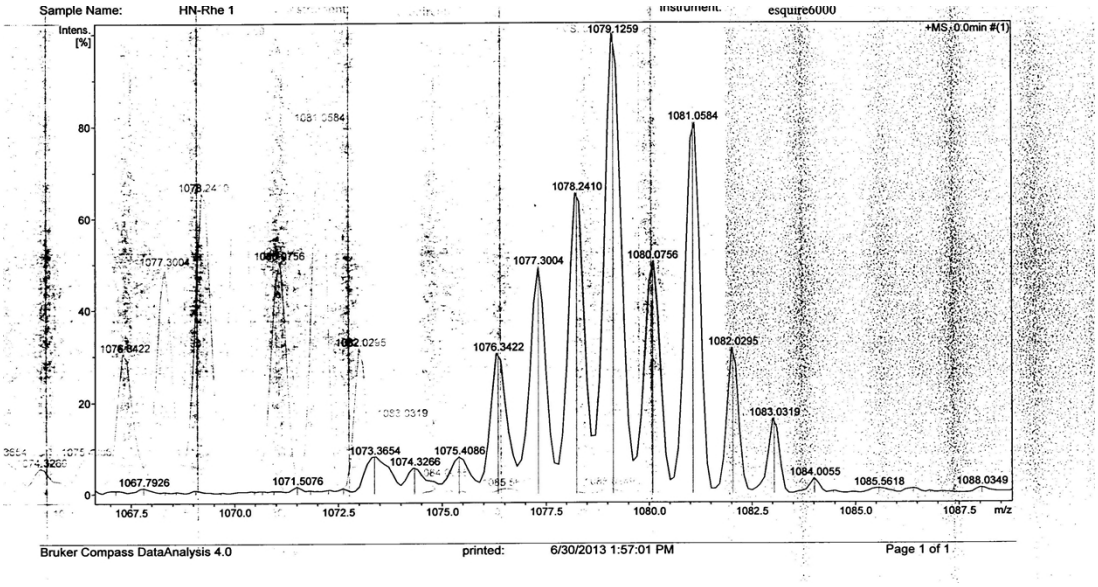

Figure S9. (a) ORTEP view of [RuCl(OH_2)(bpy)(dfppe)] cation (**9**) and selected bond lengths and bond angles

ORTEP view of the [RuCl(OH_2)(bpy)(dfppe)] (**9**) cation at the 50% probability level. Solvent and all hydrogen atoms are omitted for clarity. Selected bond lengths (Å): Ru(1)-N(2) 2.067(4), Ru(1)-N(1) 2.117(4), Ru(1)-O(1) 2.183(4), Ru(1)-P(2) 2.2392(11), Ru(1)-P(1) 2.2862(12), Ru(1)-Cl(1) 2.3722(11). Bond angles(deg): N(2)-Ru(1)-N(1) 78.57(15), N(2)-Ru(1)-O(1) 89.12(16), N(1)-Ru(1)-O(1) 78.76(15), N(2)-Ru(1)-P(2) 89.76(15), N(1)-Ru(1)-P(2) 98.73(12), O(1)-Ru(1)-P(2) 177.42(11), N(2)-Ru(1)-P(1) 100.28(11), N(1)-Ru(1)-P(1) 175.69(11), O(1)-Ru(1)-P(1) 97.09(11), P(2)-Ru(1)-P(1) 85.39(4)

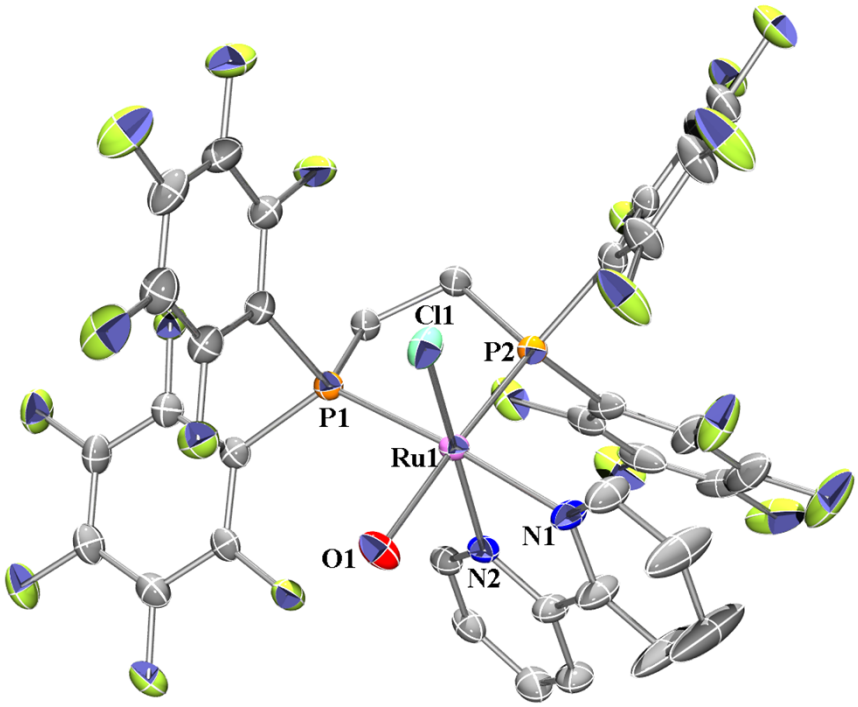

(b) ^{1}H NMR spectrum of $[RuCl(H_2O)(bpy)(dfppe)]^{+}$ (**9**) (* indicates acetone and # indicates residual water)

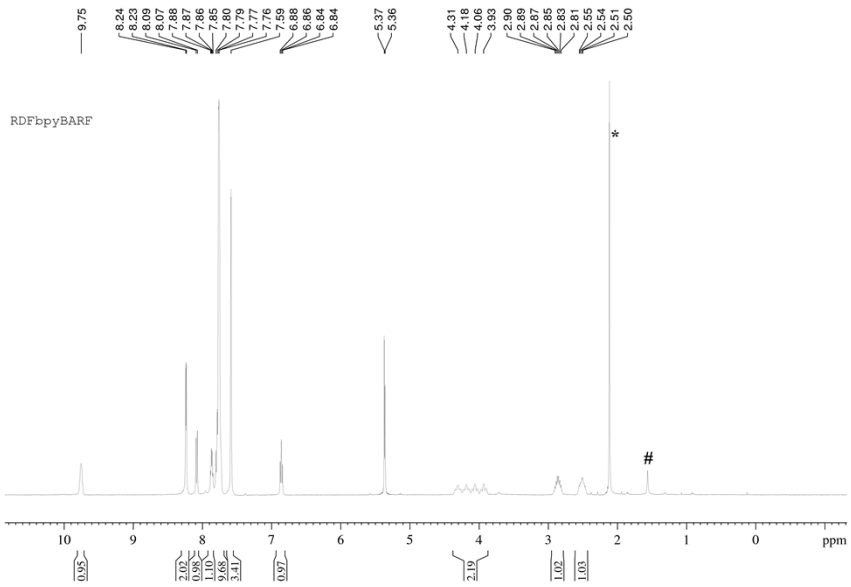

(c) ^{31}P NMR spectrum of $[RuCl(H_2O)(bpy)(dfppe)]^{+}$ (**9**)

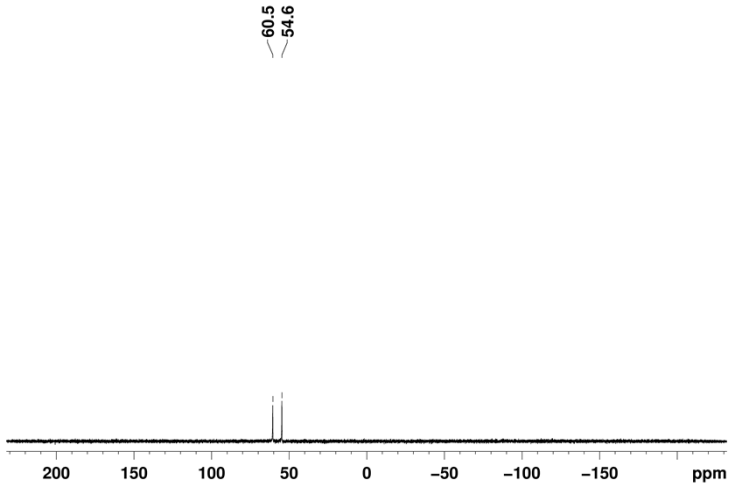

(d) ^{19}F NMR spectrum of $[RuCl(H_2O)(bpy)(dfppe)]^+$ (**9**)

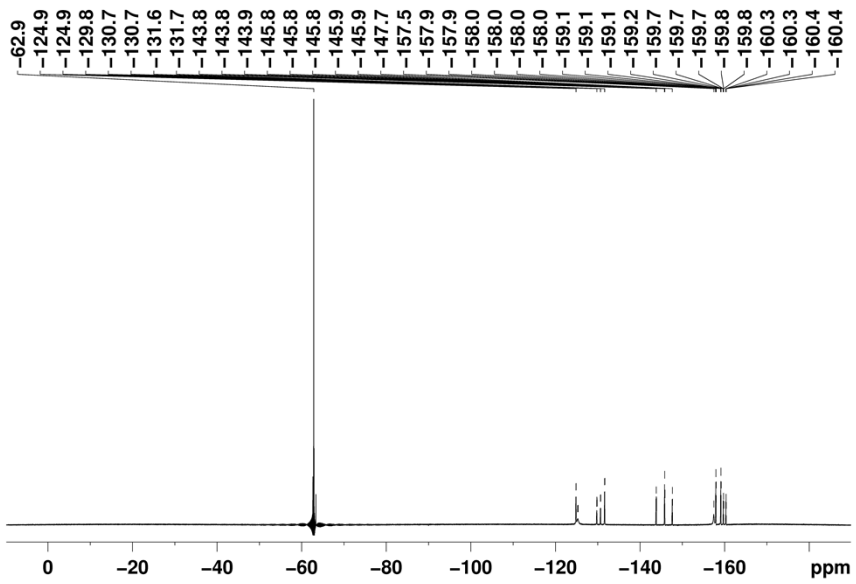

(e) ES-MS spectrum of $[RuCl(H_2O)(bpy)(dfppe)]^+$ (**9**)

Calculated Mass spectrum of (**9**)

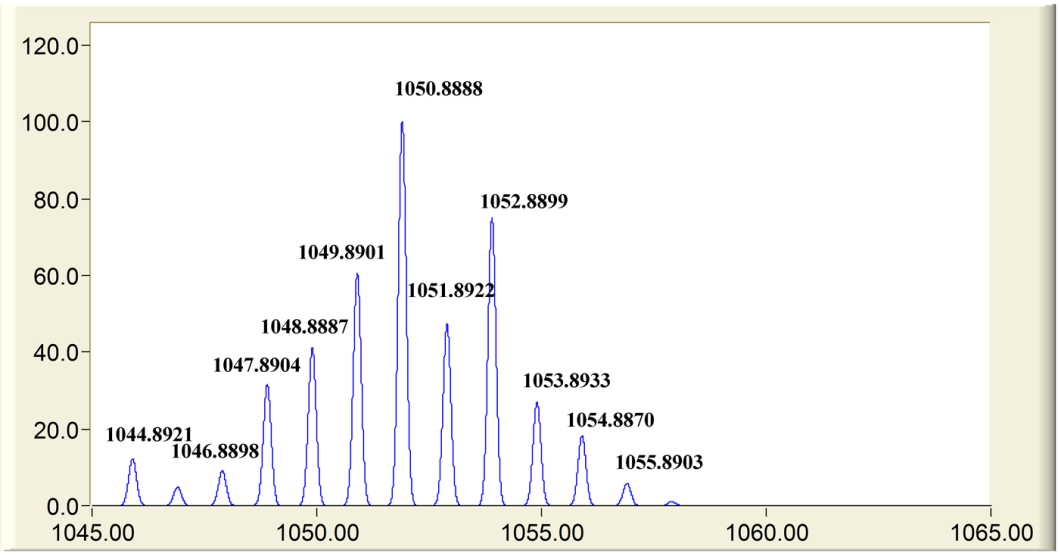

Experimental Mass spectrum of (**9**)

m/z = 1050.8873 [M^+ - (H_2O + $BAr^F{}_4^-$)]

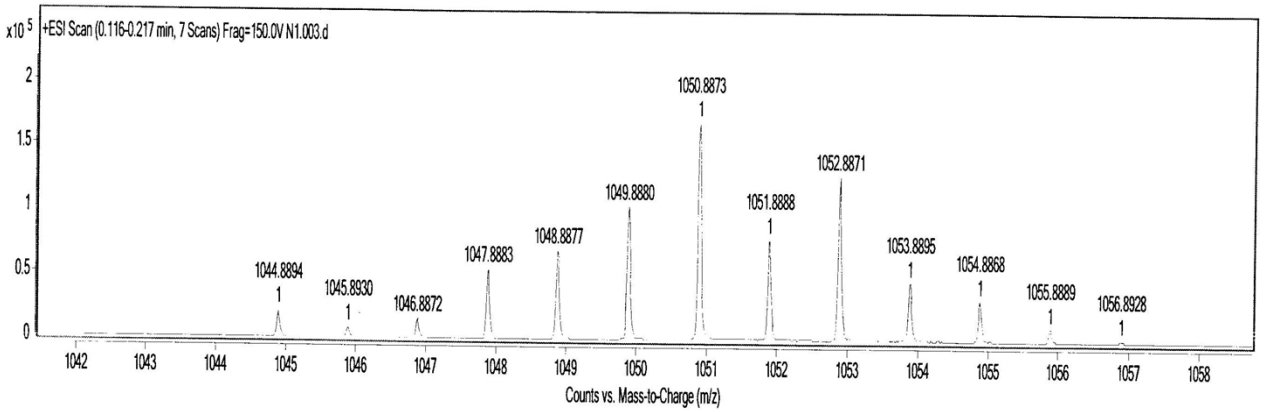

Figure S10. (a) ORTEP view of [RuH(PMe_3)(bpy)(dfppe)] cation (**10a**) and selected bond lengths and bond angles

ORTEP view of the [RuH(PMe_3)(bpy)(dfppe)] (**10a**) cation at the 50% probability level. Solvent, disorder, and all hydrogen atoms (except the Ru-H1) are omitted for clarity. Selected bond lengths (Å): Ru(1)-N(1) 2.118(5), Ru(1)-N(2) 2.174(5), Ru(1)-P(2) 2.2544(17), Ru(1)-P(1) 2.3101(16), Ru(1)-P(3) 2.3685(17), Ru(1)-H(1) 1.55(7); Bond angles(deg): N(1)-Ru(1)-N(2) 75.1(2), N(1)-Ru(1)-P(2) 173.24(14), N(2)-Ru(1)-P(2) 107.76(14), N(1)-Ru(1)-P(1) 90.96(13) N(2)-Ru(1)-P(1) 111.56(14), P(2)-Ru(1)-P(1) 82.45(6), N(1)-Ru(1)-P(3) 86.04(13), N(2)-Ru(1)-P(3) 87.07(14) P(2)-Ru(1)-P(3) 99.62(6), P(1)-Ru(1)-P(3) 159.84(6), N(1)-Ru(1)-H(1) 97(3), N(2)-Ru(1)-H(1) 169(3) P(2)-Ru(1)-H(1) 80(3), P(1)-Ru(1)-H(1) 77(3), P(3)-Ru(1)-H(1) 83(3)

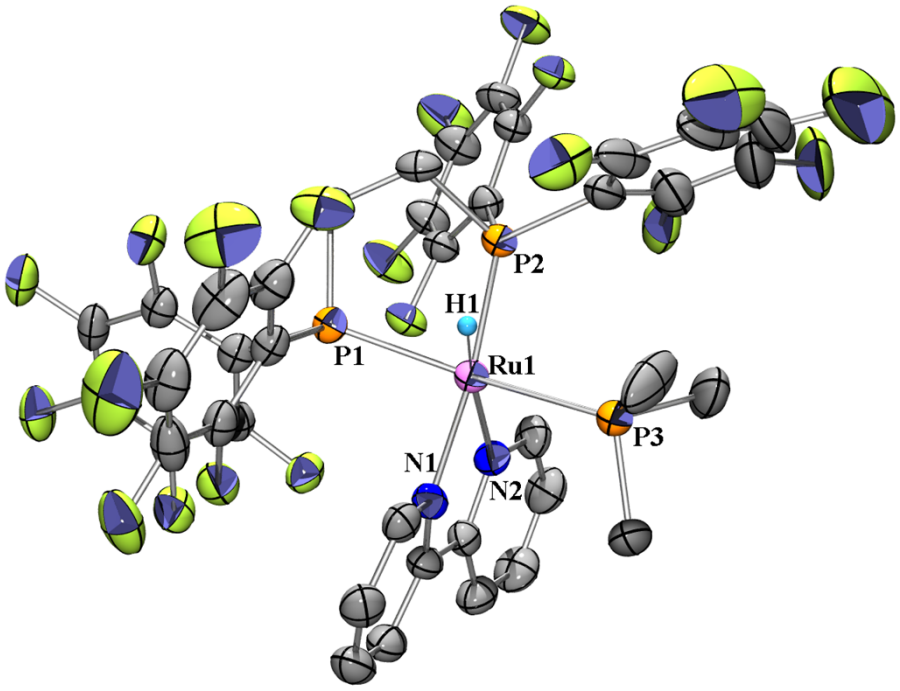

(b) ^{1}H NMR spectrum of [RuH(PMe_3)(bpy)(dfppe)]$^{+}$ (**10a**)

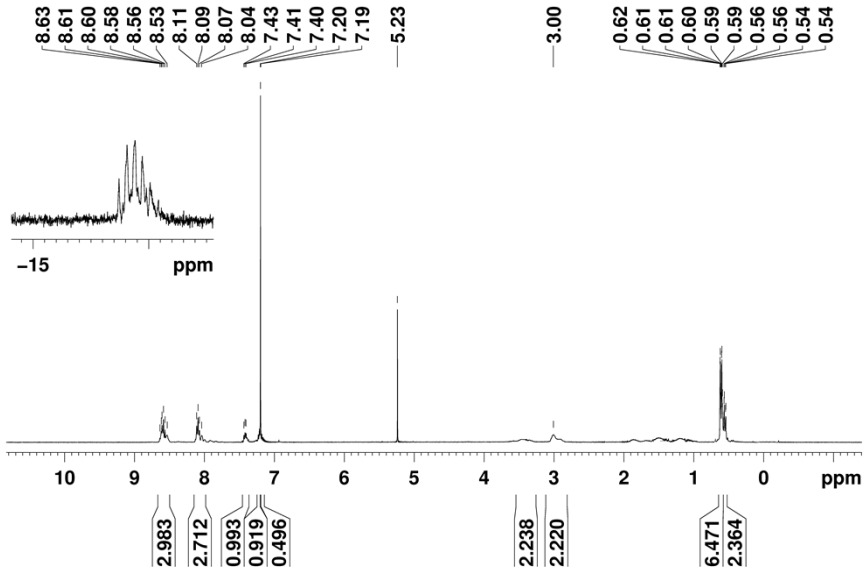

(c) ^{31}P NMR spectrum of [RuH(PMe_3)(bpy)(dfppe)]$^{+}$ (**10a**)

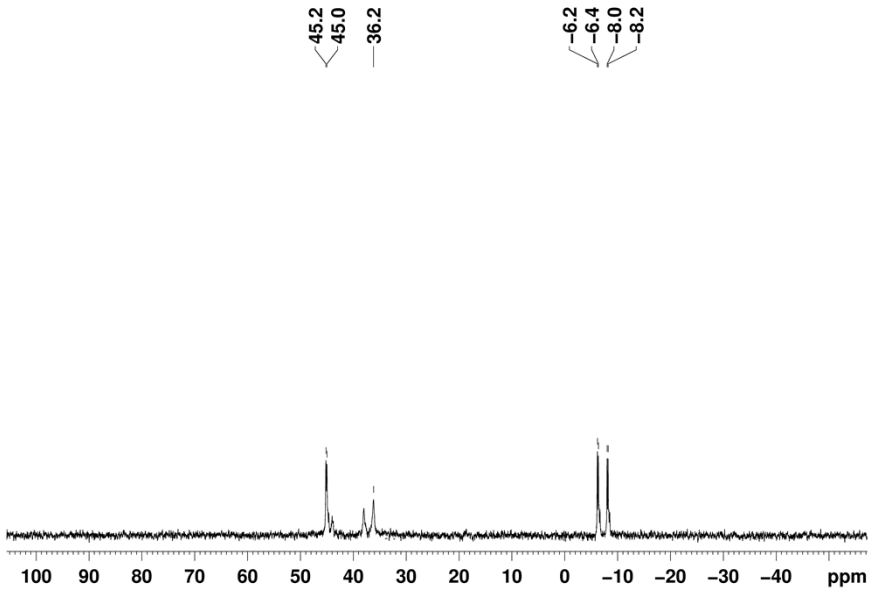

13

(d) ^{13}C NMR spectrum of $[RuH(PMe_3)(bpy)(dfppe)]^+$ (**10a**)

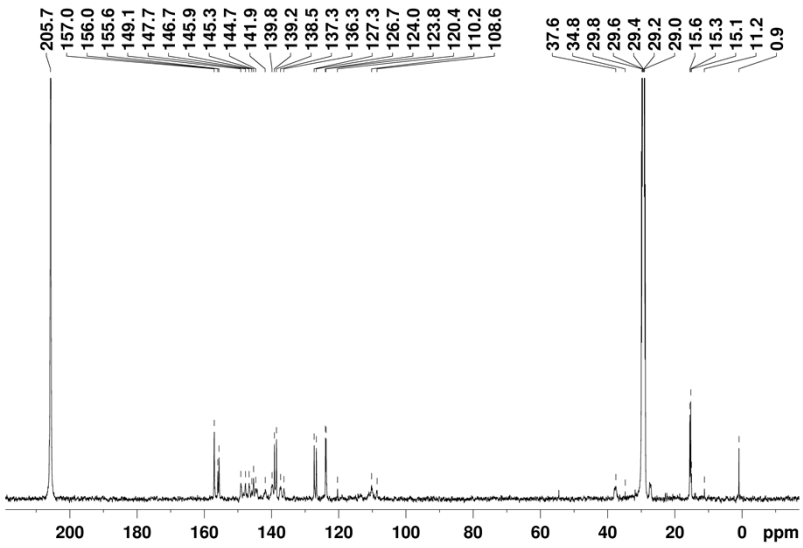

(e) ES-MS spectrum of $[RuH(PMe_3)(bpy)(dfppe)]^+$ (**10a**)

Calculated Mass spectrum (**10a**)

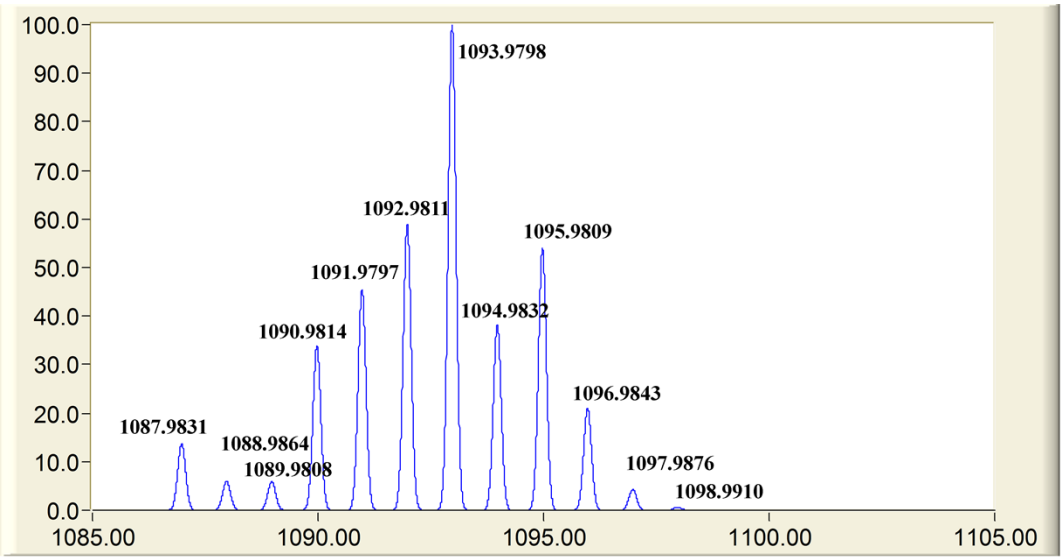

Experimental Mass spectrum of (**10a**)

m/z = 1093.1578 [(M^+ - OTf^-]

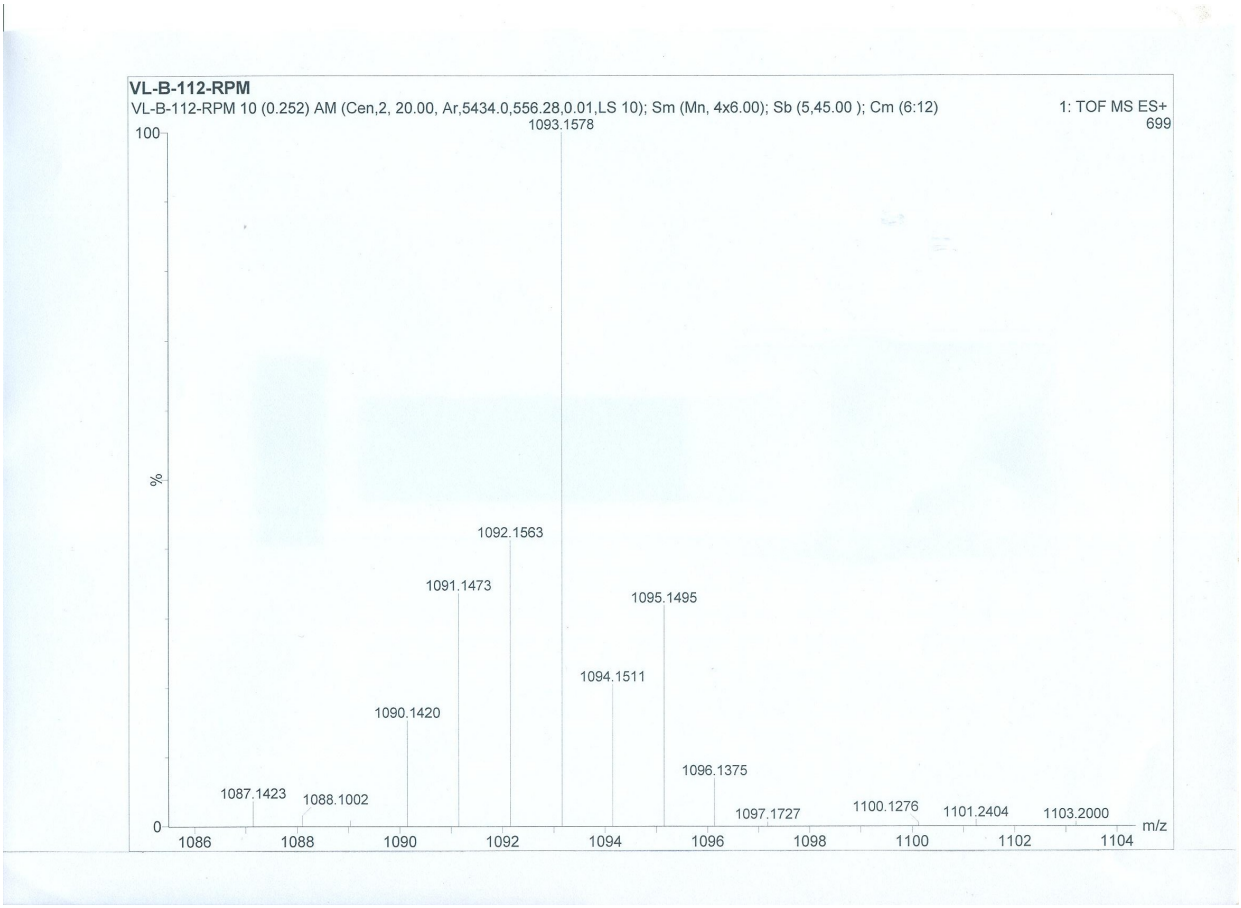

Figure S11. (a) ^{1}H NMR spectrum of $[RuH(P(OMe)_3(bpy)(dfppe)]^+$ (**11a**)

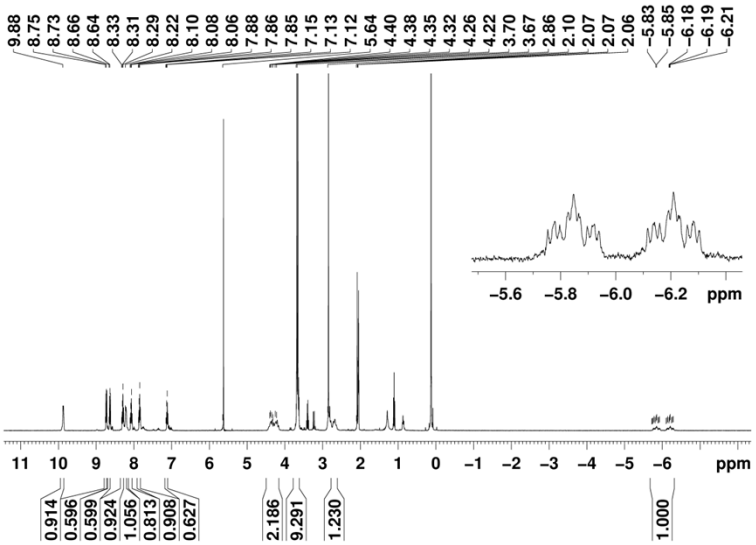

(b) ^{31}P NMR spectrum of $[RuH(P(OMe)_3(bpy)(dfppe)]^+$ (**11a**)

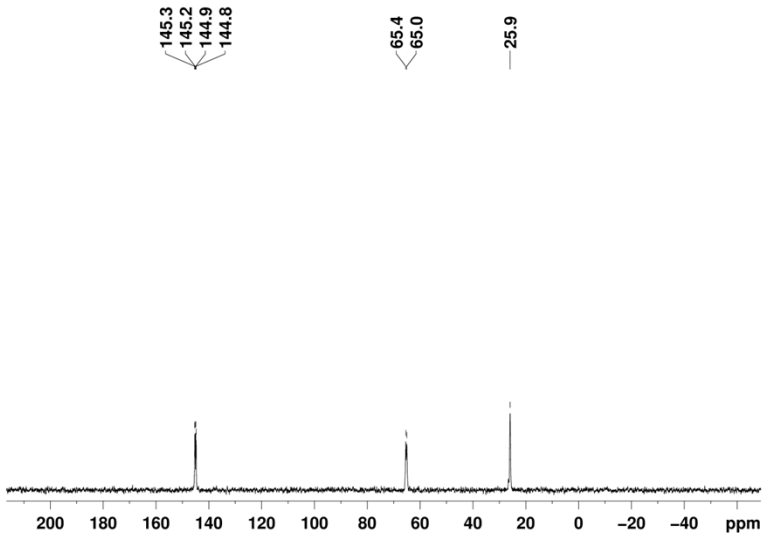

(c) ^{13}C NMR spectrum of $[RuH(P(OMe)_3(bpy)(dfppe)]^+$ (**11a**)

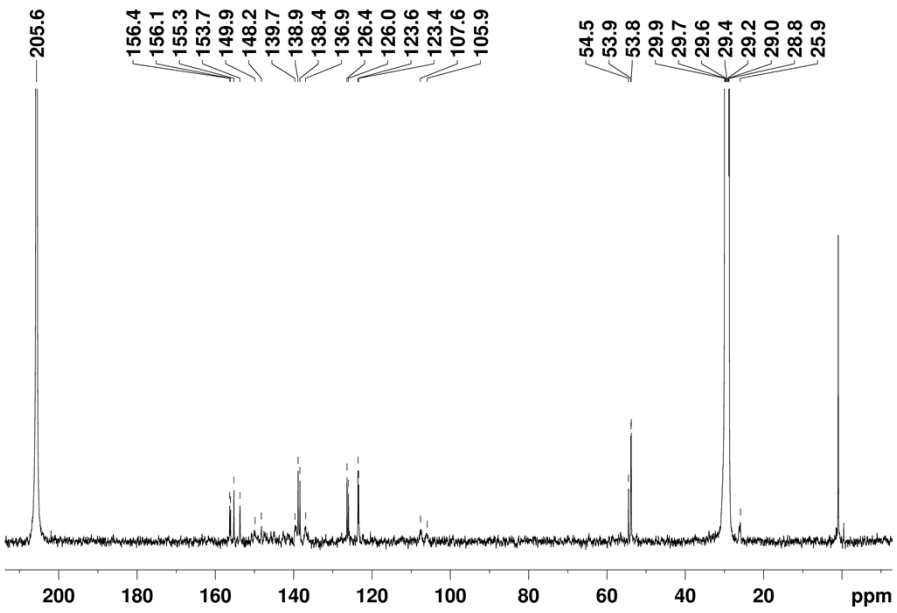

(d) ES-MS spectrum of $[RuH(P(OMe)_3(bpy)(dfppe)]^+$ (**11a**)

Calculated Mass spectrum (**11a**)

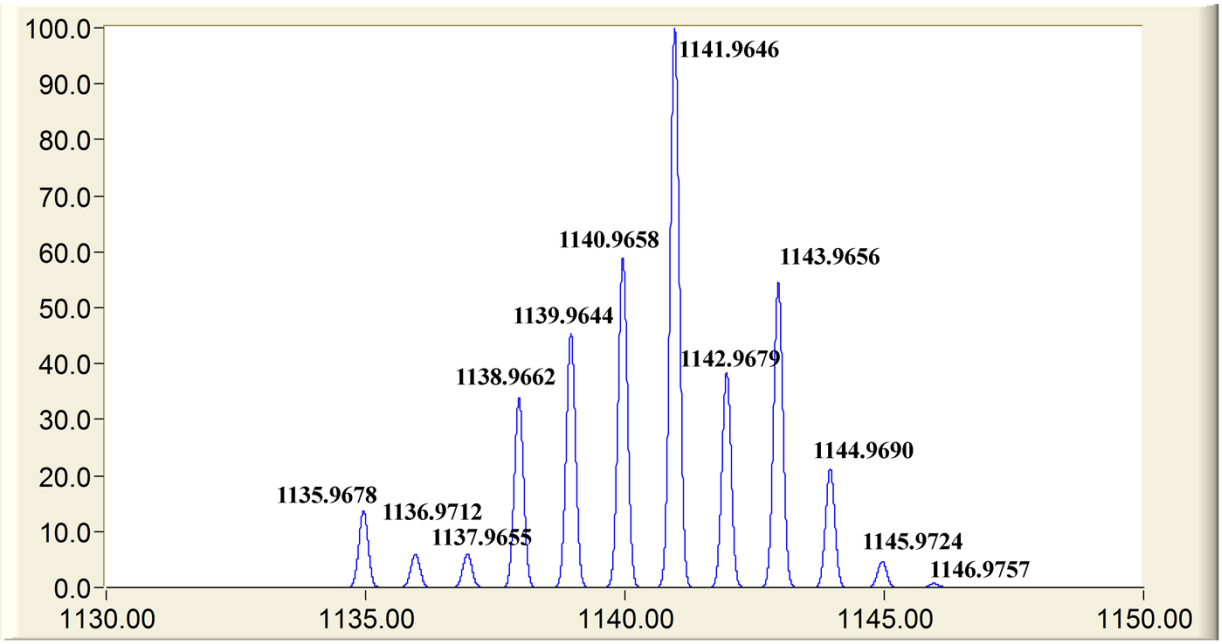

Experimental Mass spectrum of (**11a**)

m/z = 1141.2285 [$M^+ - OTf^-$]

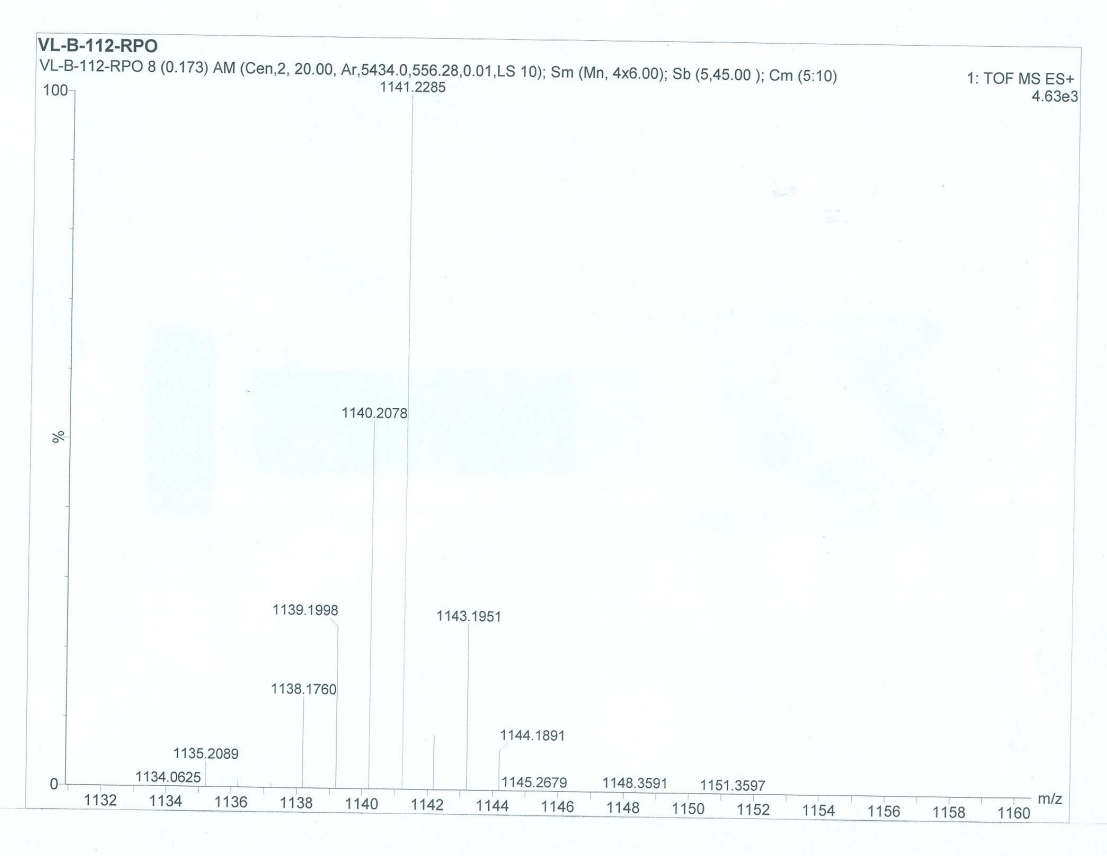

Figure S12. (a) ORTEP view of [RuH(P(OMe)$_3$)(bpy)(dfppe)] cation (**11c**) and selected bond lengths and bond angles

ORTEP view of the [RuH(P(OMe)$_3$)(bpy)(dfppe)] (**11c**) cation at the 50% probability level. Solvent and all hydrogen atoms are omitted for clarity. Selected bond lengths (Å): P(1)-Ru(1) 2.3269(11), P(3)-Ru(1) 2.2561(11), P(4)-Ru(1) 2.2681(11), Ru(1)-N(2) 2.115(4), Ru(1)-N(1) 2.184(3). Bond angles(deg): N(2)-Ru-N(1) 76.14(14), N(2)-Ru-P(3) 173.32(10), N(1)-Ru(1)-P(3) 108.57(10), N(2)-Ru(1)-P(4) 89.93(9), N(1)-Ru(1)-P(4) 84.34(9), P(3)-Ru(1)-P(4) 95.21(4), N(2)-Ru(1)-P(1) 90.93(9), N(1)-Ru(1)-P(1) 112.32(9), P(3)-Ru(1)-P(1) 82.90(4), P(4)-Ru(1)-P(1) 163.01(4)

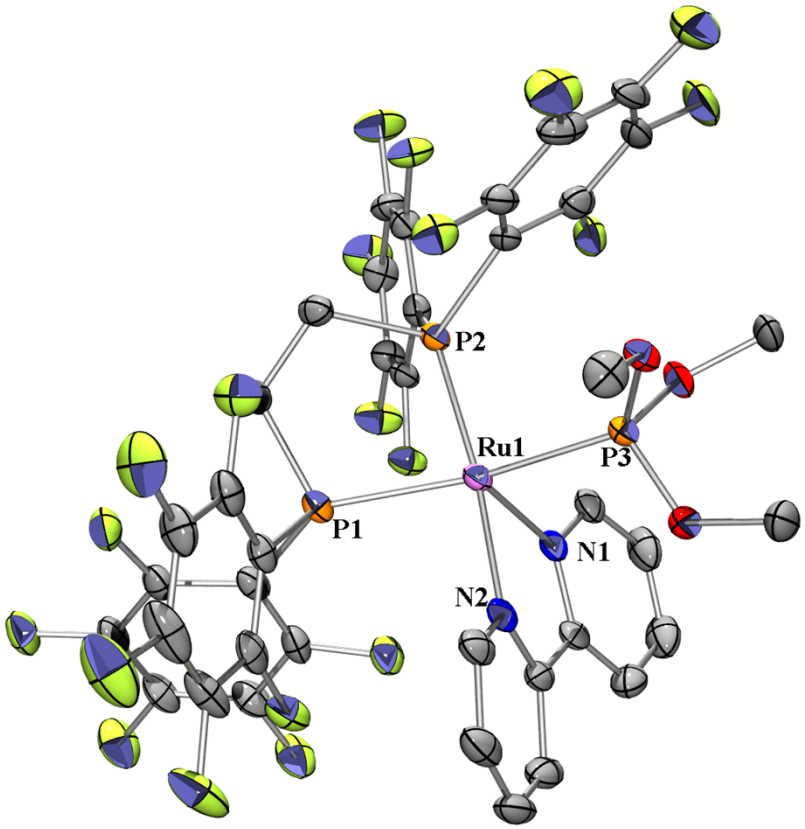

(b) ^{1}H NMR spectral stack plot (acetone-d_6, 293 K) indicating the isomerization of **11a** to **11c**

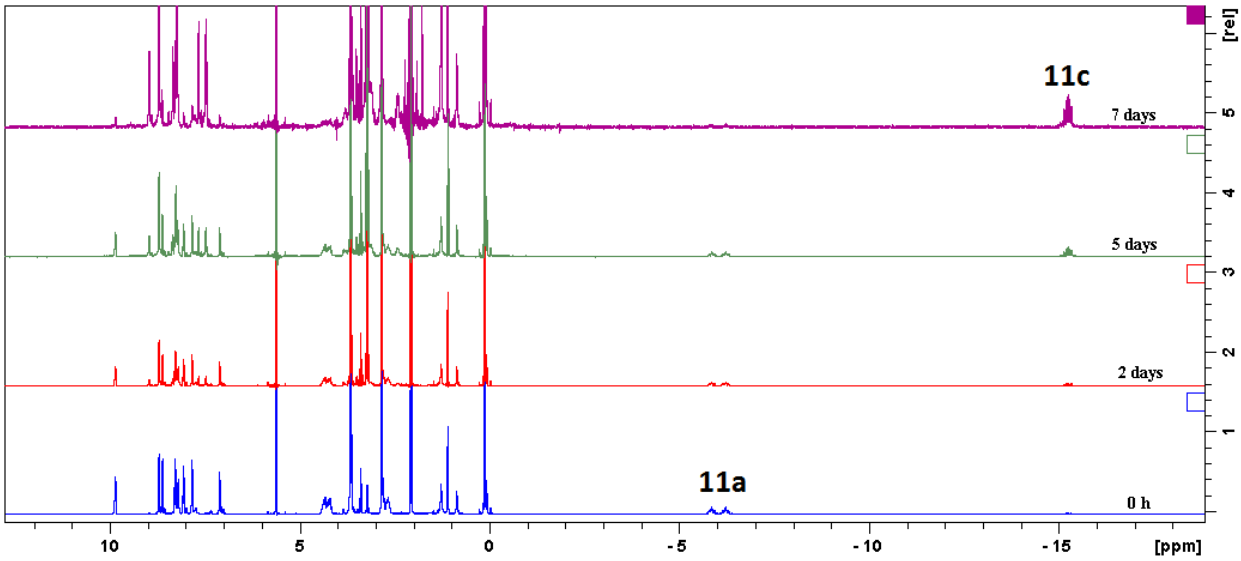

(c) $^{31}P\{^{1}H\}$ NMR spectral stack plot indicating the isomerization of **11a** to **11c**

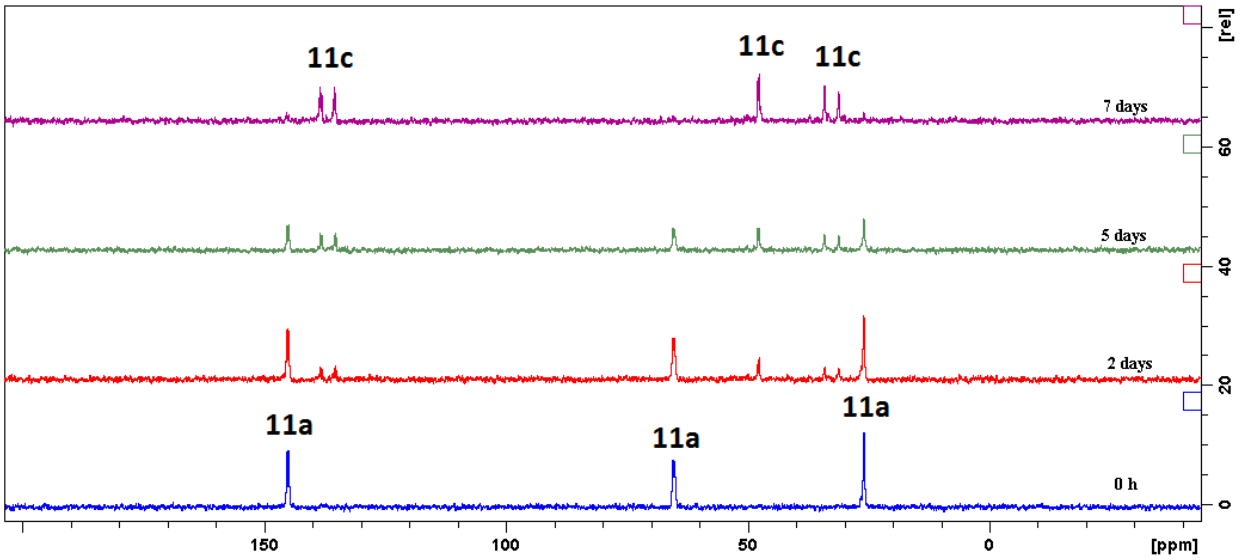

Figure S13. (a) VT ^{1}H NMR (CD_2Cl_2) spectral stack plot for the reaction of [RuH(P(OMe)$_3$)(bpy)(dfppe)][OTf] with HOTf.

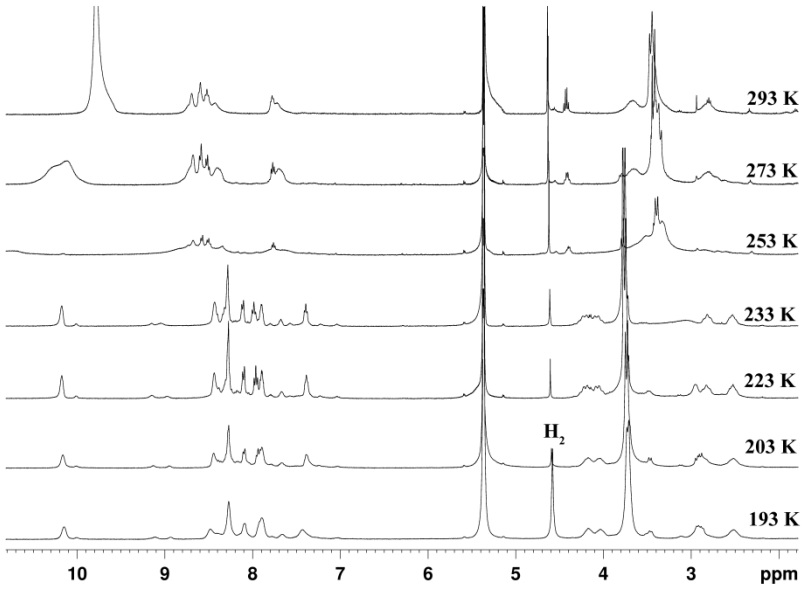

(b) VT $^{31}P\{^{1}H\}$ NMR (CD_2Cl_2) spectral stack plot for the reaction of [RuH(P(OMe)$_3$)(bpy)(dfppe)][OTf] with HOTf .

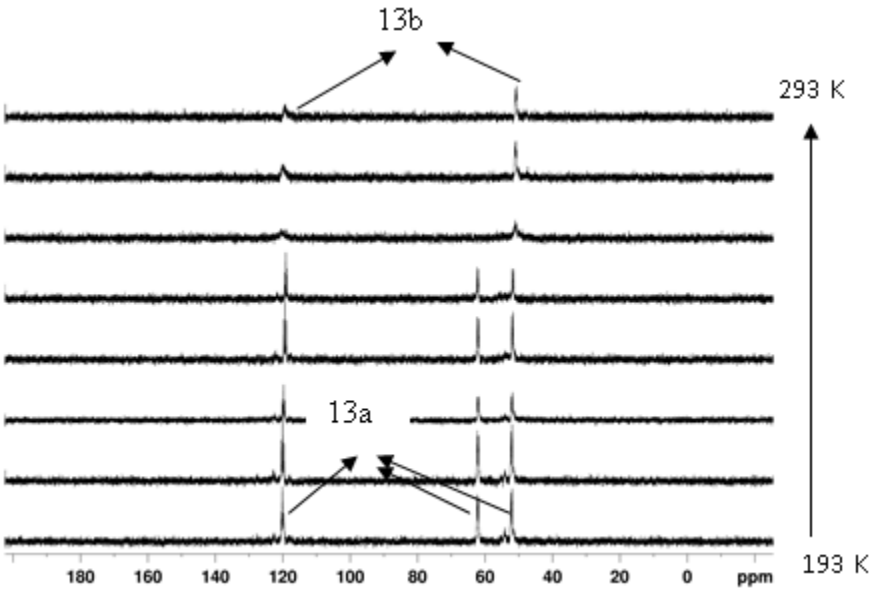

(c) VT $^{31}P\{^{1}H\}$ NMR (CD_2Cl_2) spectral stack plot for the reaction of hydride complex, [RuH($P(OMe)_3$)(bpy)(dfppe)][OTf] with HOTf.

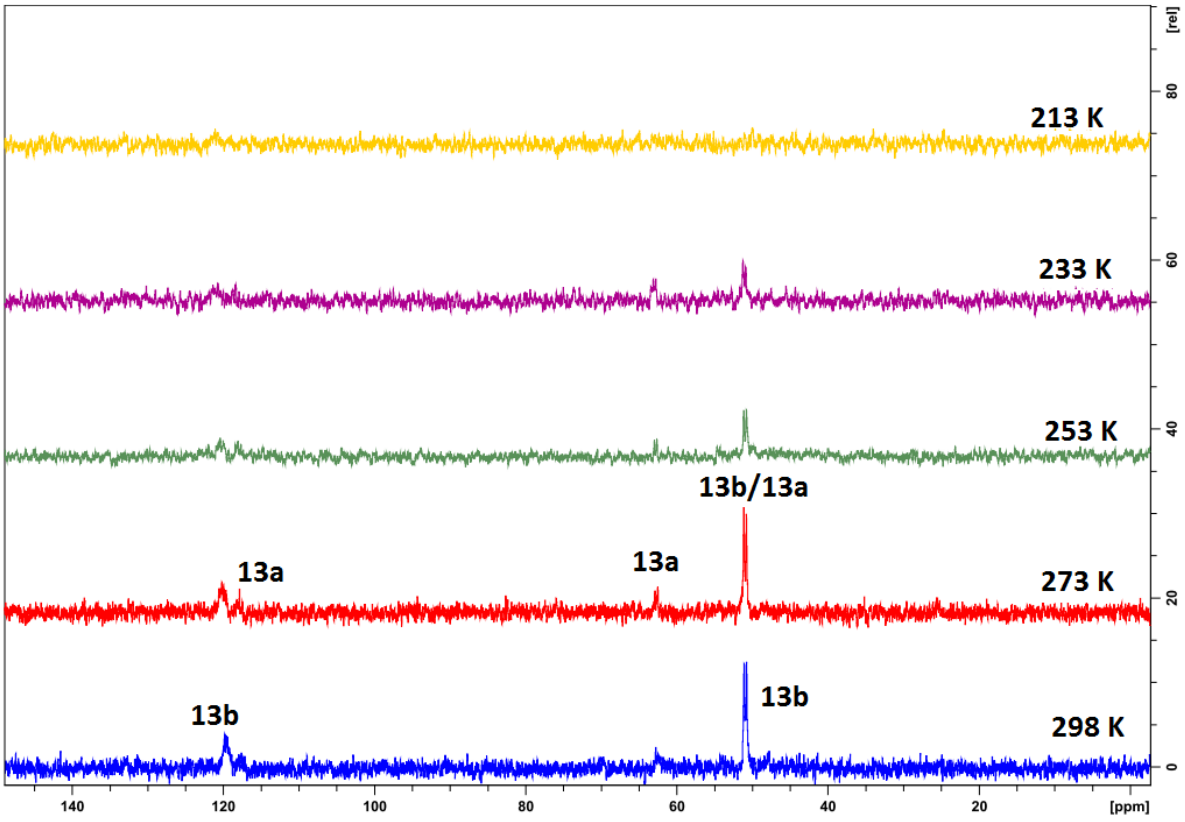

(d) VT ^{19}F NMR spectral stack plot for the reaction of hydride complex, $[RuH(P(OMe)_3)(bpy)(dfppe)][OTf]$ with HOTf.

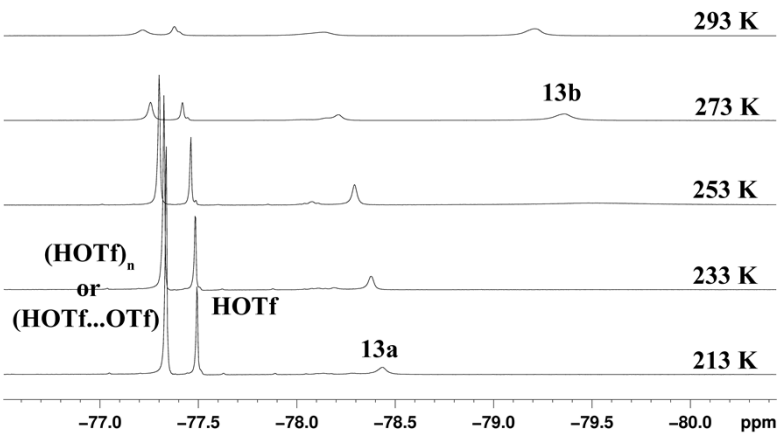

(e) Spin-saturation transfer experiment: ^{31}P NMR spectral stack plots for the reaction of hydride complex, $[RuH(P(OMe)_3)(bpy)(dfppe)][OTf]$ with HOTf (irradiation of **13a**)

Spin-saturation transfer Experiment

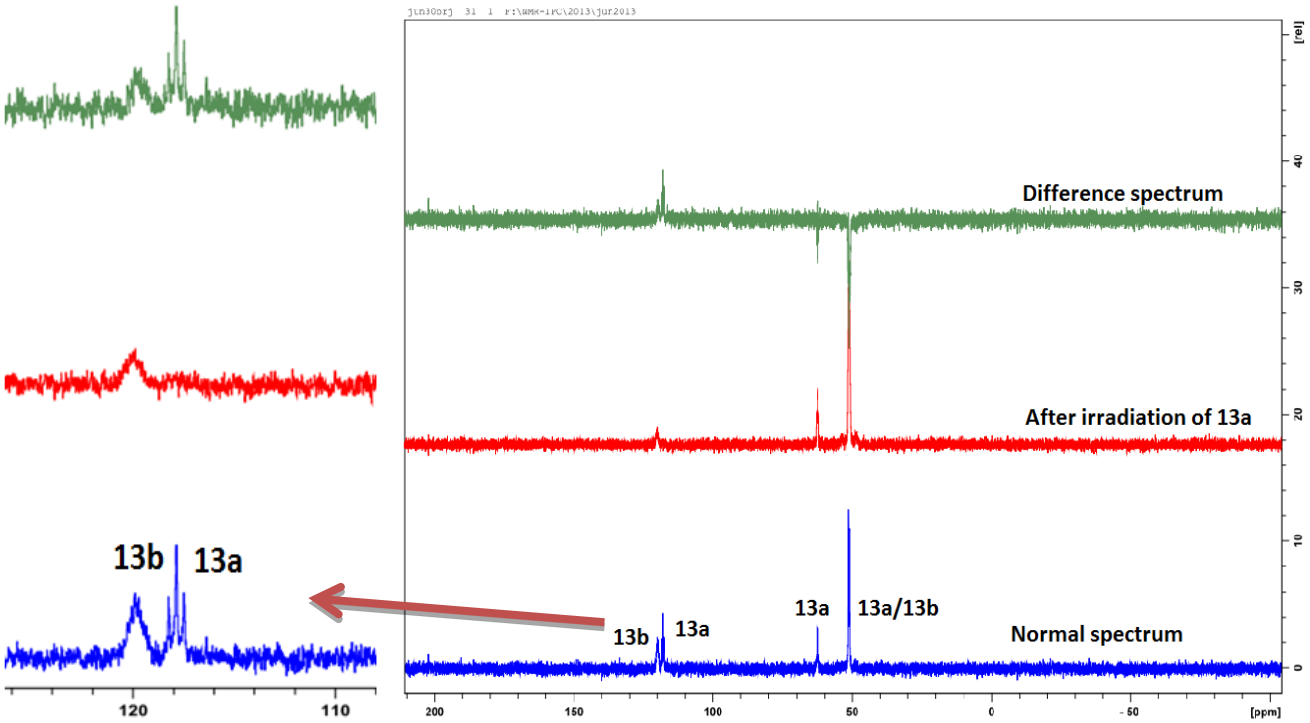

Figure S14. (a**)** ^{1}H NMR spectrum of isomeric aqua complex (acetone-d_6, 293 K) $[Ru(H_2O)(P(OMe)_3)(bpy)(dfppe)][OTf]_2$ (**14a** (85 %), **14b** (15 %)) (in the expansion coordinated water signals of isomers, * denotes residual water in acetone–d_6 and # denotes hexane and silicone grease peak)

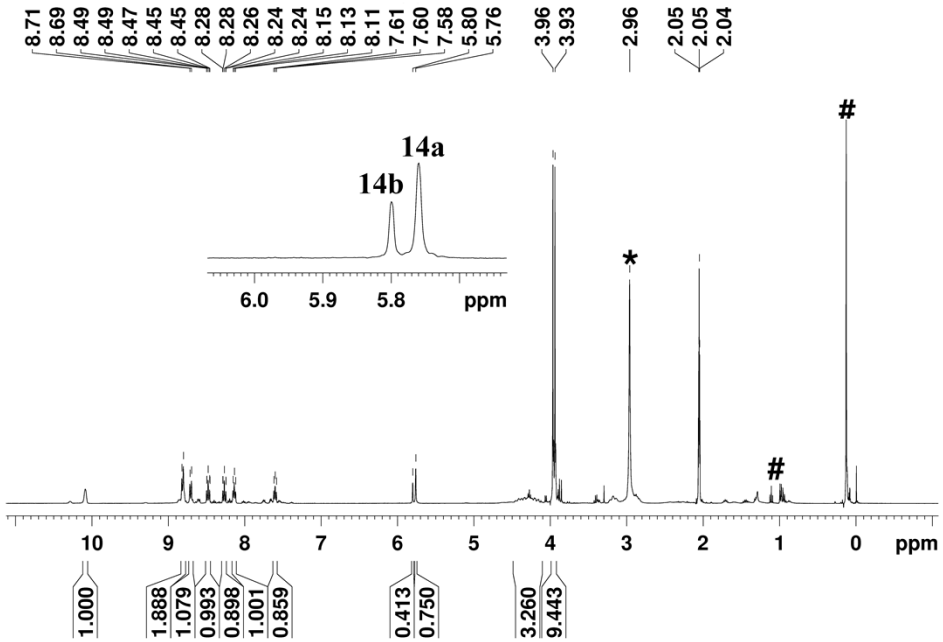

(b) $^{31}P\{^{1}H\}$ NMR (acetone-d_6, 293 K) spectrum of isomeric aqua complex $[Ru(H_2O)(P(OMe)_3)(bpy)(dfppe)][OTf]_2$ (**14a** (85 %), **14b** (15 %))

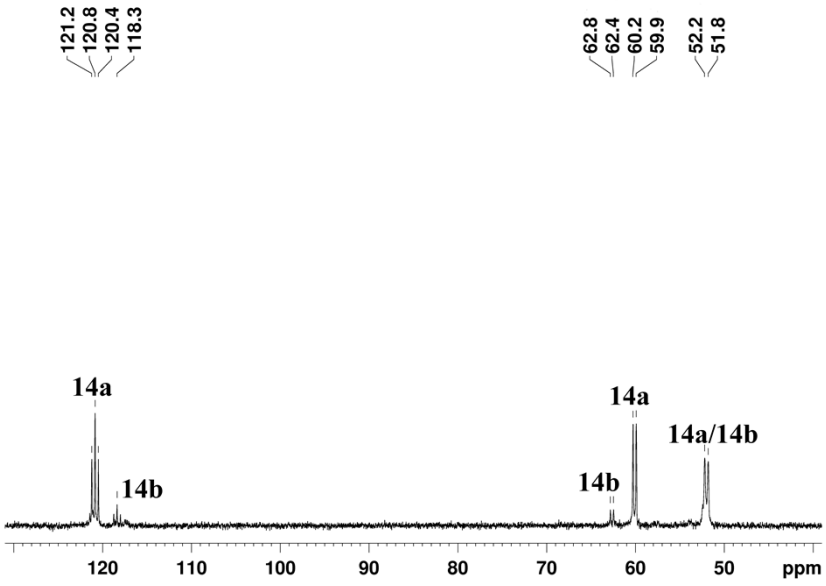

(c) IR spectrum of $[Ru(H_2O)(P(OMe)_3)(bpy)(dfppe)][OTf]_2$ (**14a**, **14b**), [ν (H_2O)] = 3520 cm^{-1}.

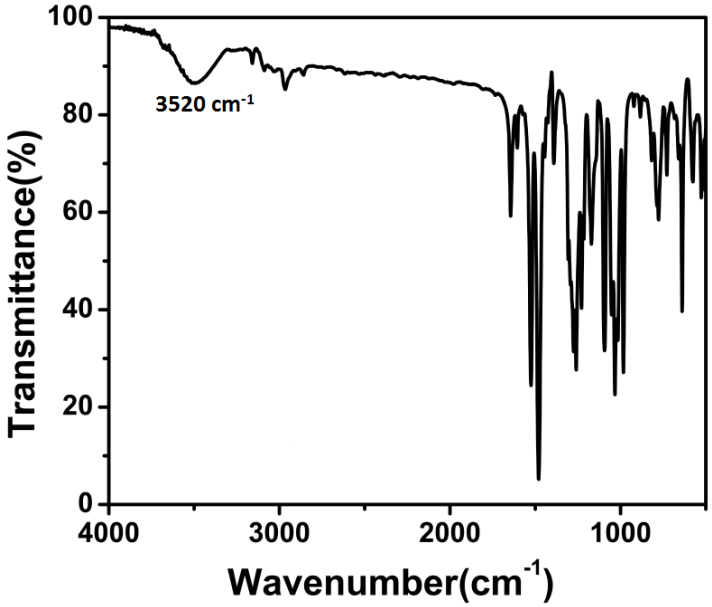

(d) ^{13}C NMR (acetone-d_6, 293 K) spectrum of isomeric aqua complex $[Ru(H_2O)(P(OMe)_3)(bpy)(dfppe)][OTf]_2$ **14a** (85 %), **14b** (15 %))

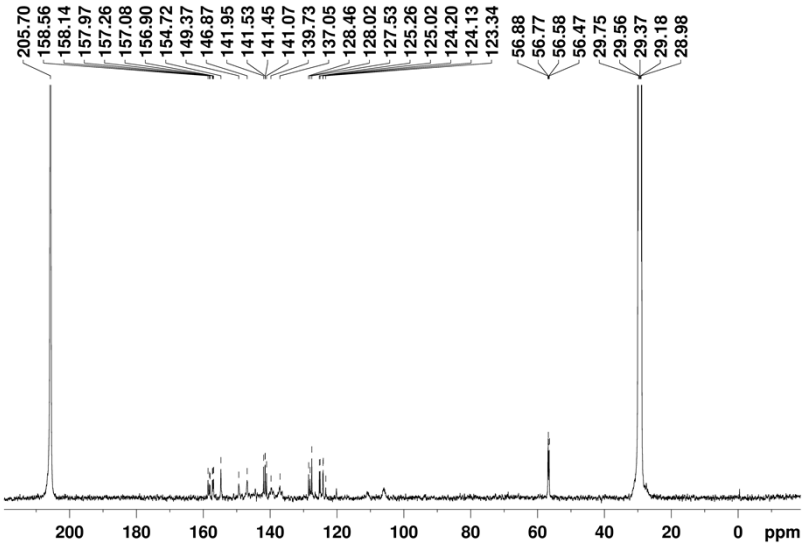

(e) ES-MS spectrum of isomeric aqua complexes $[Ru(H_2O)(P(OMe)_3)(bpy)(dfppe)][OTf]_2$ **14a** (85 %), **14b** (15 %)

Calculated Mass spectrum of (**14a**, **14b**)

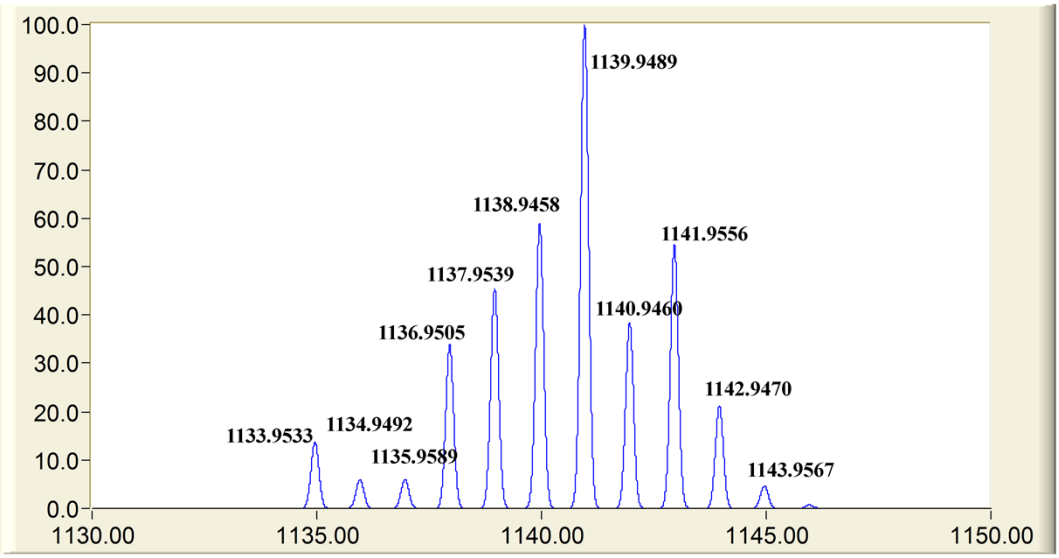

Experimental Mass spectrum (**14a**, **14b)**

m/z = 1136.9460 $[M^+ - (H_2O + 2OTf^-)]$

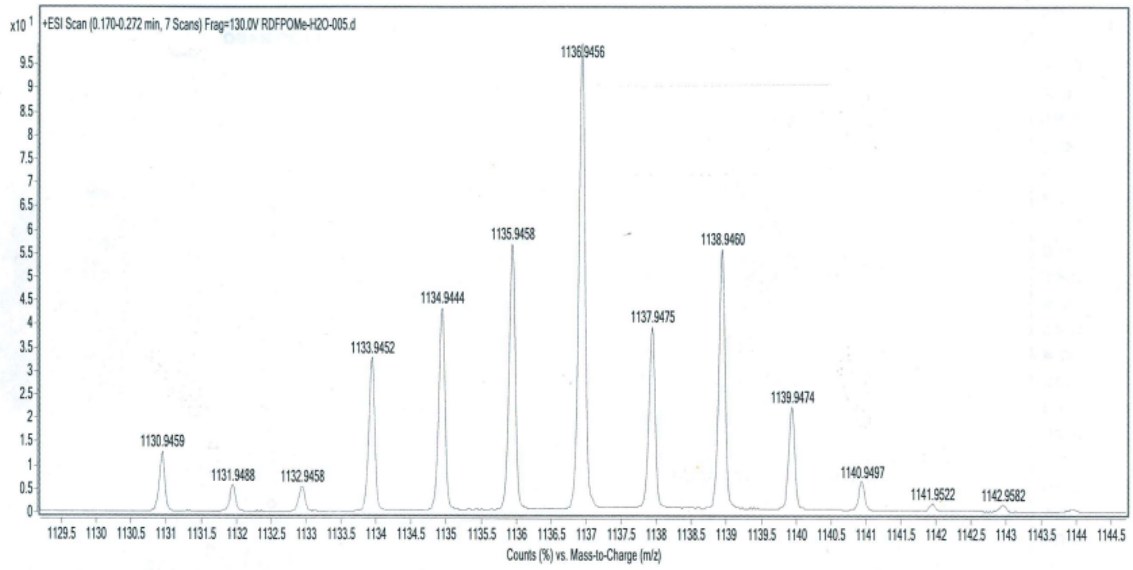

Figure S15. (a) ^{1}H NMR spectral stack plot for the reaction of $[Ru(H_2O)(P(OMe)_3)(bpy)(dfppe)][OTf]_2$ (**14a**, **14b**) with H_2. (acetone-d_6, 293 K)

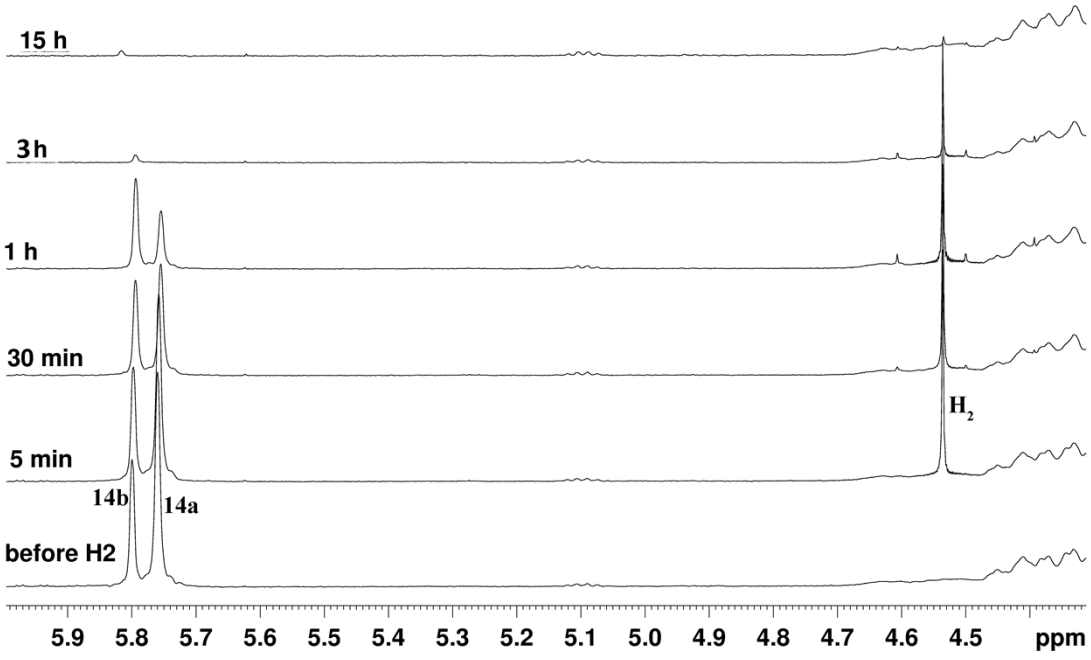

(b) $^{31}P\{^{1}H\}$ NMR spectral stack plot for the reaction of $[Ru(H_2O)(P(OMe)_3)(bpy)(dfppe)][OTf]_2$ (**14a**, **14b**) with H_2 (acetone-d_6, 293 K)

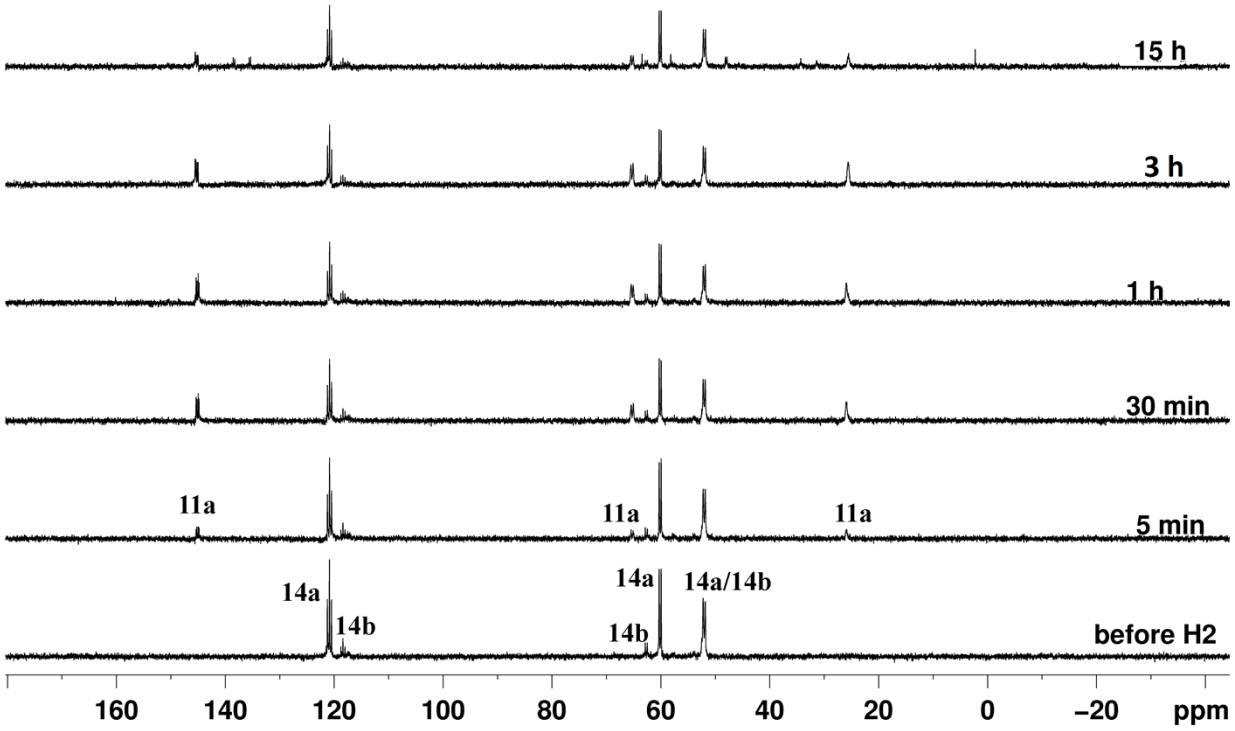

Figure S16. ^{2}H NMR spectrum of $[Ru(D)(P(OMe)_3)(bpy)(dfppe)][OTf]$(**11a-*d***) in acetone-d_6 at 293 K.

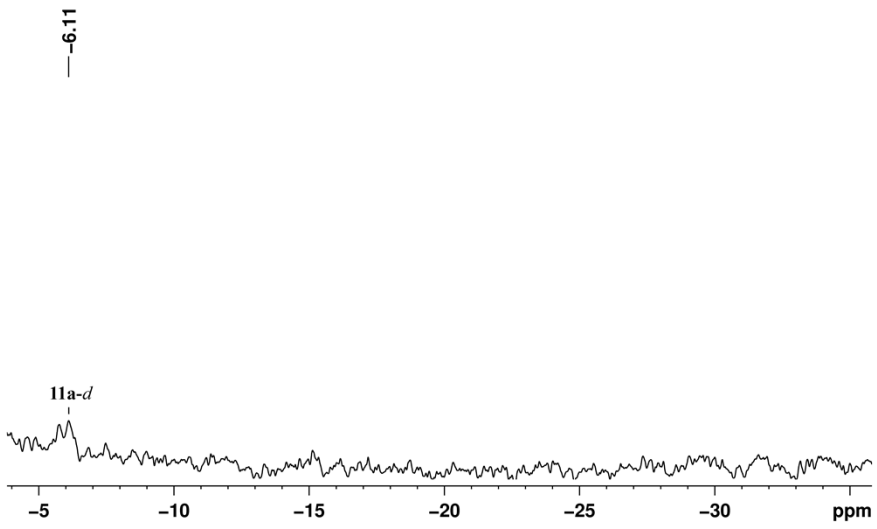

Figure S17. (a) ^{1}H NMR spectrum of $[Ru(NCCH_3)(P(OMe)_3)(bpy)(dfppe)][OTf]_2$ (**15**) (acetone-d_6, 293 K)

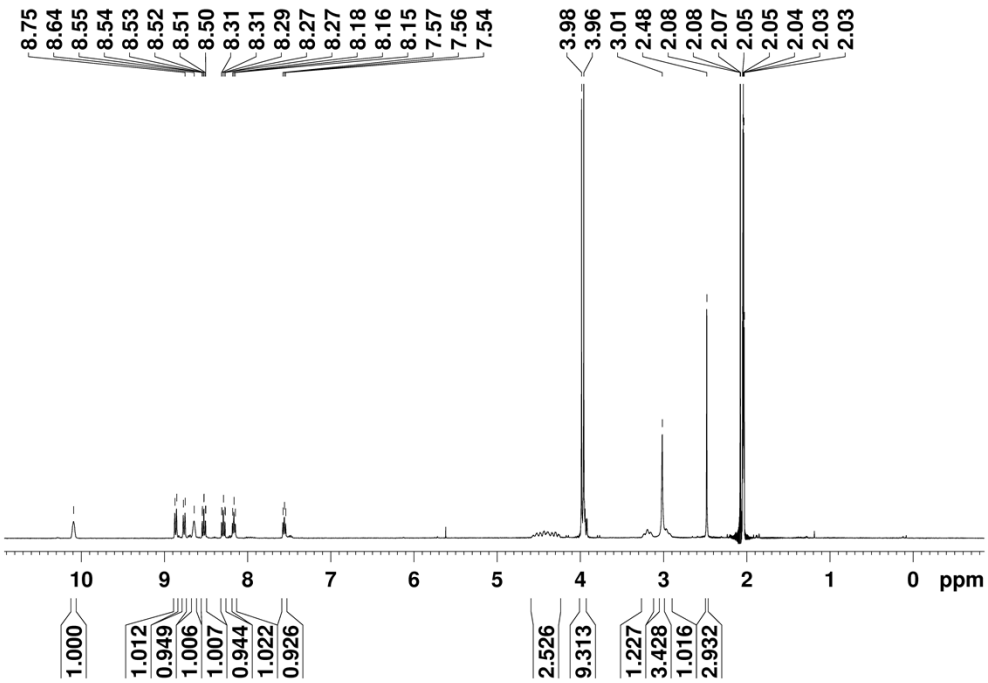

(b) $^{31}P\{^{1}H\}$ NMR spectrum of $[Ru(NCCH_3)(P(OMe)_3)(bpy)(dfppe)][OTf]_2$ (**15**) (acetone-d_6, 293 K)

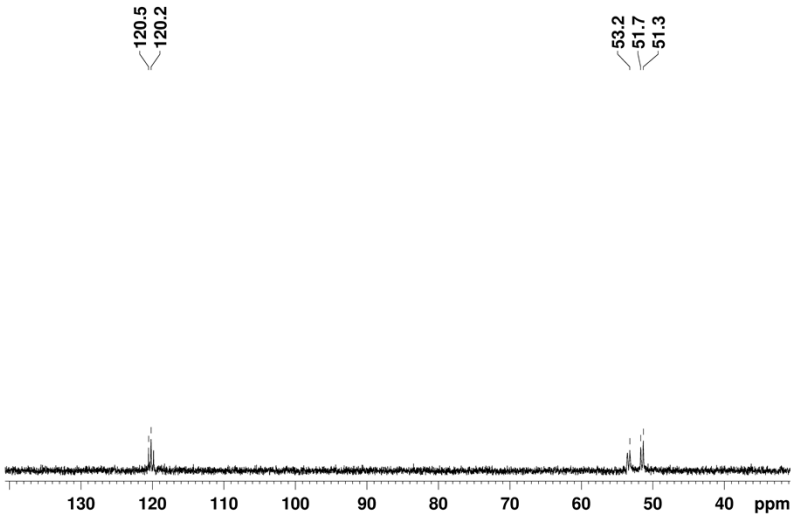

(c) ^{13}C NMR spectrum of $[Ru(NCCH_3)(P(OMe)_3)(bpy)(dfppe)][OTf]_2$ (**15**) (acetone-d_6, 293 K)

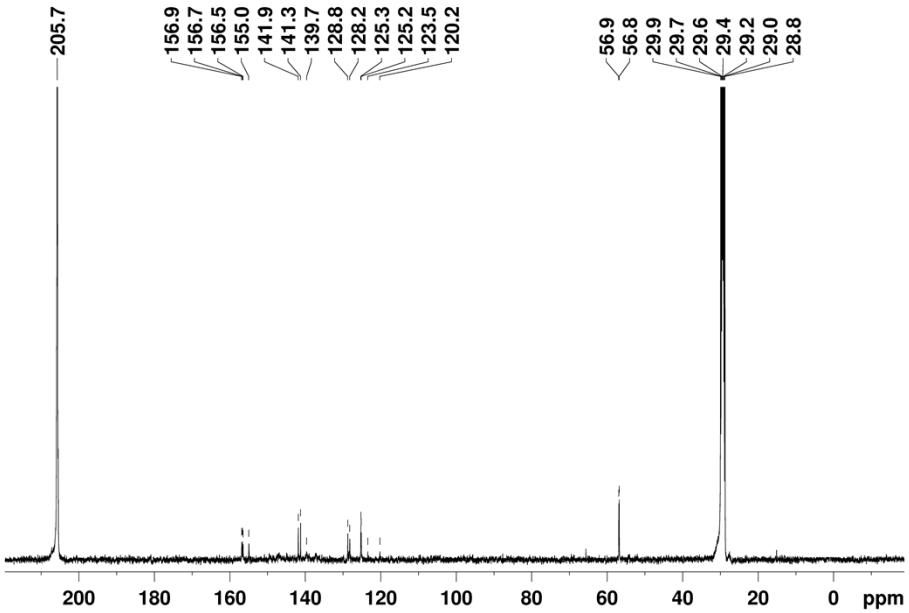

(d) ES-MS spectrum of $[Ru(NCCH_3)(P(OMe)_3)(bpy)(dfppe)][OTf]_2$ (**15**)

Calculated Mass spectrum (**15**)

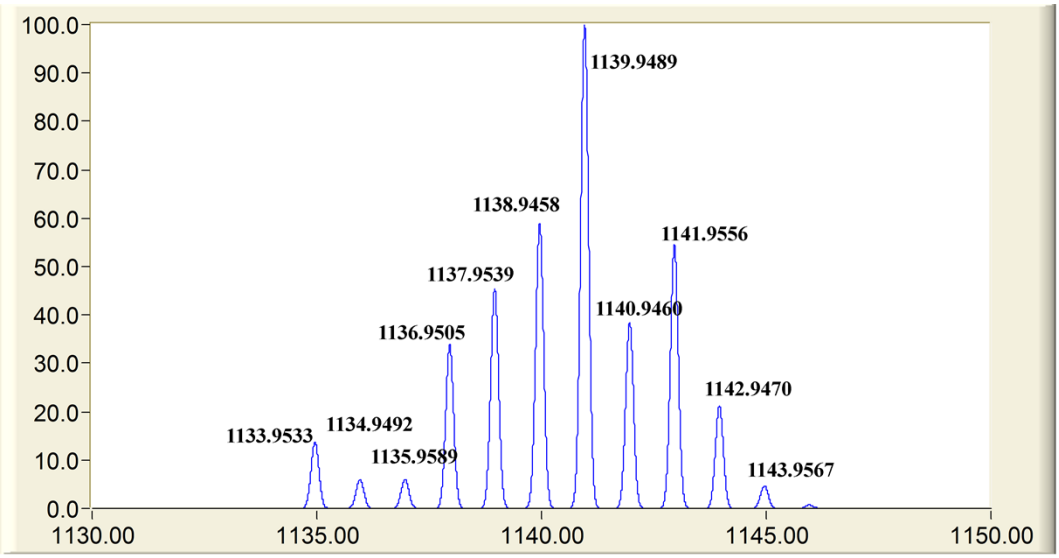

Experimental Mass spectrum (**15**)

m/z = 1137.2452 [M^+ –CH_3CN - 2OTf^-]

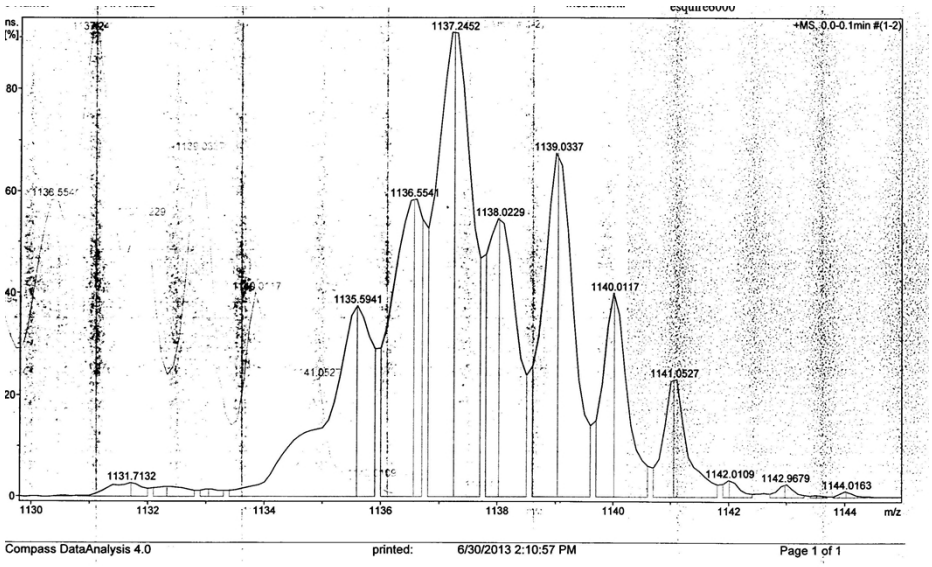

Table 2. Experimental elemental analysis data sheet along with a table for the compounds **11a**, **14**, **5**, **7**, **10**, **9**, **4**, **11c**, **8**.

Details of CHNS/O Elemental Analysis:

Instrument:
Model: Thermo Scientific Flash 2000 Organic Elemental Analyzer
Analysis Mode: CHNS/O Mode
Software: Eager Experience

Experimental Conditions:
Detector: Thermal Conductivity Detector
Carrier gas: He
Reference gas: He
Column: CHNS/NCS column PQS SS 2M 6X5 mm in oven at 75° C (for CHNS)
Column: SS 1M 6X5mm (MS 5A) in oven at 100°C (for oxygen)
Adsorption trap material: Soda lime and Anhydrone

Program:
CHNS furnace temp (°c): 950
Oxygen furnace temp (°c): 1060
Oven temp (°c): 65
Oven run time (Sec): 720 sec (for CHNS)
350 sec (for Oxygen)
Carrier gas flow (mL/min): 140
Oxygen gas flow (mL/min): 250
Reference gas flow (mL/min): 100
Sampling delay (sec): 12
Oxygen Injection end (sec): 5
Auto zero: on
Detector gain: 1

	% Nitrogen	%Carbon	%Hydrogen	% Sulphur
11a.RDFP(OMe)H	1.92287993	36.23170499	2. 33469280	2.34678349
14.RDFPOH2O	1.63986143	32.93152512	1.61904263	4.34425015
5.RDFP(OMe)3Cl	2.13552674	34.99147464	1.35317707	2.32345218
7.RDFACN	3.42162358	37.52667999	1.43859979	2.60893421
10.Rdfpme3h	2.19349897	37.34367852	2.42743436	2.34286476
9.Rdfbarf	1.24456732	41.24905268	1.64834521	
4.Rdfphen	2.52784532	40.26674239	1.34865342	
11c. Rdfbpynh	2.01754376	36.19657643	1.82745362	2.43764294
8. rdfcocl	2.43896541	37.24176390	1.27237890	2.51345265

Table 3. Experimental elemental analysis data sheet along with a table for the compounds **2**, **1**, **6**, **3**.

Details of CHNS/O Elemental Analysis:

Instrument:
Model: Thermo Scientific Flash 2000 Organic Elemental Analyzer
Analysis Mode: CHNS/O Mode
Software: Eager Experience

Experimental Conditions:
Detector: Thermal Conductivity Detector
Carrier gas: He
Reference gas: He
Column: CHNS/NCS column PQS SS 2M 6X5 mm in oven at 75° C (for CHNS)
Column: SS 1M 6X5mm (MS 5A) in oven at 100°C (for oxygen)
Adsorption trap material: Soda lime and Anhydrone

Program:
CHNS furnace temp (°c): 950
Oxygen furnace temp (°c): 1060
Oven temp (°c): 65
Oven run time (Sec): 720 sec (for CHNS)
350 sec (for Oxygen)
Carrier gas flow (mL/min): 140
Oxygen gas flow (mL/min): 250
Reference gas flow (mL/min): 100
Sampling delay (sec): 12
Oxygen Injection end (sec): 5
Auto zero: on
Detector gain: 1

	% Nitrogen	%Carbon	%Hydrogen	% Sulphur
2. rdfcl		34.78562687	1.23372346	
1. rdfdmso		28.78544563	2.23543763	9.12564478
6.rdfpme3cl	2.13675435	40.63678943	2.32128654	2.14789435
3.rdfbpycl	2.01967125	32.73656738	1.08435762	

Table 4. Experimental elemental analysis data sheet along with a table for the compounds **6**, **9**.

Details of CHNS/O Elemental Analysis:

Instrument:
Model: Thermo Scientific Flash 2000 Organic Elemental Analyzer
Analysis Mode: CHNS/O Mode
Software: Eager Experience

Experimental Conditions:
Detector: Thermal Conductivity Detector
Carrier gas: He
Reference gas: He
Column: CHNS/NCS column PQS SS 2M 6X5 mm in oven at 75° C (for CHNS)
Column: SS 1M 6X5mm (MS 5A) in oven at 100°C (for oxygen)
Adsorption trap material: Soda lime and Anhydrone

Program:
CHNS furnace temp (°c): 950
Oxygen furnace temp (°c): 1060
Oven temp (°c): 65
Oven run time (Sec): 720 sec (for CHNS)
350 sec (for Oxygen)
Carrier gas flow (mL/min): 140
Oxygen gas flow (mL/min): 250
Reference gas flow (mL/min): 100
Sampling delay (sec): 12
Oxygen Injection end (sec): 5
Auto zero: on
Detector gain: 1

	% Nitrogen	%Carbon	%Hydrogen	% Sulphur
C-6-rpme3cl	2.19434121	40.21573326	2.62845212	2.21732213
C-9.rdfbarf	1.33643728	41.63764321	1.64286432	